DR (G CUNNINGHAM
S 959
IS DEPARTMENT OF THE INTERIOR
EOLOGICAL SURVEY
ESTON VA 22092

OFFICIAL BUSINESS
ENALTY FOR PRIVATE USE $300

Earth Science
in the
Public Service

RESTON
JUL 21 '93
VA

PENALTY FOR PRIVATE USE $300
01.67
METER

PRIORITY
AIR MAIL

MR KEN HAZEN
BOX 12
RICO CO 81332

United States Department of the Interior
GEOLOGICAL SURVEY
RESTON, VA 22092

July 21, 1993

Dear Ken,

I enjoyed meeting you in Rico during my last visit — thanks for the beautiful prints!

As promised, I am enclosing copies of the scientific reports that have been published about Rico during recent years. Peter Larson, myself, and Chuck Naeser have been working there now for about 15 years — hardly seems possible.

Thanks again for your kindness —

Sincerely,

Skip Cunningham

SOCIETY OF
MINING ENGINEERS
OF
AIME
CALLER NO. D, LITTLETON, COLORADO 80127

PREPRINT
NUMBER
85-118

DISCOVERY OF THE SILVER CREEK MOLYBDENUM DEPOSIT RICO, COLORADO

Larry F. Barrett
Donald E. Cameron
John C. Wilson

Anaconda Minerals Company
Denver, Colorado

For presentation at the SME-AIME Annual Meeting
New York, New York - February 24-28, 1985

Abstract. Anaconda exploration in the Rico mining district from 1978 through early 1983 resulted in discovery and partial definition of the Silver Creek molybdenum deposit. Approximately 44 million tons of 0.31% Mo are drill-indicated, and projections suggest that the deposit exceeds 200 million tons. No source intrusion has been intersected by drilling, but its composition is suggested by silicic alkali-alaskite porphyry dikes of intramineral age observed at the surface and in drill holes.

Age data and fluid inclusion studies indicate that the deposit was formed 5.2 ±2 m.y. ago and that more than 1,200 meters of cover has since been removed by erosion.

Both emplacement of the hypothesized source intrusion, and the geometry of the molybdenum deposit, were influenced by three major intersecting faults. The most significant of these, the Last Chance fault, juxtaposes Precambrian quartzite and greenstone against Pennsylvanian clastic and calcareous sediments within the mineralized zone.

Wallrock alteration associated with the deposit is characterized by potassic, phyllic, and propylitic zones in non-calcareous rocks, and garnet and anhydrite-diopside zones in the carbonates. All +0.2% Mo mineralization is within the potassic and garnet zones.

Pre-mineral faults that intersect the deposit contain the only surficial molybdenum, tungsten, and fluorine anomalies. Pervasive dispersion haloes of the indicator elements were intersected at depth by drilling in the discovery phase of exploration, and are particularly well-developed in the hanging wall of the Last Chance fault.

Introduction

Rico is an historic lead-zinc silver mining district located in the San Juan Mountains of southwestern Colorado at elevations ranging from 2,700 to 3,800 meters (Figure 1). Mining from veins and from replacement deposits in calcareous sediments produced 83,847 tons of lead, 82,717 tons of zinc, 5,637 tons of copper, 14,513,288 ounces of silver and 83,045 ounces of gold from 1879 through 1968 (McKnight, 1974, p. 6). Production ceased in 1971 with the closure of the Blaine mine, which directly overlies the Silver Creek molybdenum deposit.

Anaconda acquired an interest in the district in 1978 and aggressively explored for porphyry and replacement deposits through early 1983. These efforts resulted in the discovery of the Silver Creek deposit, a possible world class molybdenum resource.

History of the Silver Creek Discovery

The discovery of the Silver Creek molybdenum deposit resulted from application of the Climax-type molybdenum porphyry model to a structurally complex, sediment-dominated host environment. Intangible requirements for success were an economic environment conducive to high-risk exploration, persistence and innovation by the geologic staff, and unprecedented management dedication. Without any one of these ingredients a discovery may not have been made.

Anaconda optioned a major portion of the Rico district in 1978 to explore and develop high grade copper, silver and gold replacement deposits similar to the NBH Zone (Figure 2), which had been discovered near Silver Creek by Crystal Oil two years earlier.

The NBH Zone was open to the north and east, and was the focus of the initial study, but the Anaconda task force that evaluated the district in 1978 concluded that a larger, copper porphyry target existed about 2 kilometers north of Silver Creek. This target was never tested, however, because a new team assigned to the project in 1979 recognized potential for discovery of the molybdenum deposit in Silver Creek.

Several of Crystal Oil's drill holes were analyzed for molybdenum, tungsten, and fluorine by the new exploration team, and one of these, a 529 meter hole in Silver Creek about 600 meters west of the Silver Creek deposit, showed increases in tungsten and fluorine with depth. This hole was correctly inferred to have intersected the periphery of a porphyry molybdenum system and this interpretation was the basis for locating Anaconda's first completed drill hole, C-25 (Figure 3). C-25 was positioned near the intersection of the Last Chance and Blackhawk faults to test for: 1)extensions of the NBH Zone; and 2)a porphyry center from which the NBH was thought to be laterally zoned. C-25 drifted about 230 meters southwest away from the fault intersection where it would have encountered better grades, but did intersect very strong fluorine and tungsten gradients and significant molybdenum (15 meters of 0.064% Mo) that were correlated with data from the outer margin of the Henderson deposit (Ranta et. al., 1976; Wallace et. al., 1978).

Step-out drilling followed the geologic success of C-25, but it wasn't until 7 holes later that C-30 intersected 226 meters of .106% Mo and provided essential encouragement to continue exploration drilling. C-30 had been started early in the step-out program but had been stopped in May, 1980, at 358 meters, when it began to drift toward C-25. It was re-entered and deflected in 1981 as a last attempt to locate the deposit.

Drill hole SC-1 intersected better grades late in 1981 and indicated that the center of the system lies farther southeast under the steep slopes of Blackhawk Mountain. The adit level of the Blaine mine was rehabilitated to provide winter access, and exploration was transferred to the underground in November, 1981. Holes SC-5 and SC-6, drilled from underground, obtained excellent intercepts (SC-5 intersected 194 meters of 0.334% Mo).

The encouraging results from SC-5 and SC-6 justified inception of prefeasibility studies, but it soon became apparent that development was not warranted under extant market conditions. As a last effort before ceasing exploration, drill hole SC-7a was deflected southeast from SC-5 to obtain a large step-out, and to attempt to verify that the deposit was both large and high grade. It succeeded in indicating size potential, but like previous

holes it failed to locate the center of the system. This drill hole intersected 87 meters of 0.29% Mo (0.2% Mo cutoff) and significantly expanded the drill-indicated tonnage of the deposit. The exploration program at Rico was discontinued in February, 1983.

Geology of the Silver Creek Area

The Rico mining district is centered on the Rico dome, a Laramide uplift cored by Precambrian rocks and flanked by a thick section of Paleozoic sediments (Figure 3). The Silver Creek molybdenum system probably constitutes the mineralization center of the district. A thermal center that coincides with the Silver Creek system was recognized independently by Naeser (1979), using progressively reset fission track ages on mineral separates from Laramide intrusions to establish locations of major late-Tertiary heat sources.

Stratigraphy

The Precambrian section (Figure 4) consists of a phyllitic Proterozoic greenstone unit comprised of flows and intrusions that is unconformably overlain by orthoquartzites of the Uncompahgre Formation. The orthoquartzites are generally white and massive, but locally contain intercalated argillaceous layers. The Precambrian rocks are the principal hosts of the drill-indicated molybdenum mineralization.

Mississippian Leadville Limestone as thick as 75 meters generally overlies the Uncompahgre Formation. Karst features and erosional alteration recognized within the Leadville indicate that it was exposed to erosion prior to deposition of the Hermosa Group. The Leadville hosts the NBH copper-silver-gold deposit and may host tungsten-rich tactites intersected by C-25.

The Pennsylvanian Hermosa Group is a thick sequence of clastic and calcareous sediments that has three members (Cross and Spencer, 1900). Limey shales predominate in the lower member and limestones are most abundant in the middle member. Limestones of the middle member host most of the district's known lead-zinc-silver mineralization. The upper member of the Hermosa Group is predominately clastic. The Pennsylvanian Molas Formation may be locally present at the base of the Hermosa Group, but is included in the lower member of the Hermosa for illustrative purposes.

The Hermosa Group is overlain on the fringes of the district by redbeds of the Pennsylvanian Rico and Permian Cutler Formations. These formations are not significantly mineralized and may have been too high in the section to have been reached by ascending mineralizing fluids.

Intrusive rocks include the Rico monzonite stock (78 m.y., fission track, sphene; Naeser et. al., 1979), exposed in the western part of the district; abundant dikes and sills of hornblende latite porphyry (59.9-64.9 m.y., fission track, zircon; Naeser et. al., 1979); and rare dikes of silicic alkali-alaskite porphyry (3.4-3.9 m.y., fission track, zircon, Naeser et. al., 1979). One of several alaskite dikes intersected by drill hole SC-1 was analyzed (Table 1) and age-dated by the authors at 5.2 ±0.2 m.y. (K-Ar whole rock). This dike is clearly intramineral and is probably a differentiate of the source stock.

The very young age of the Silver Creek intrusion may account for elevated geothermal gradients noted in the district (Medlin, E., 1983, personal communication). Gradients in the Silver Creek area average about 3.8°C/100 meters of depth.

Structure

The Last Chance, Blackhawk and Princeton faults (Figures 5 and 6) are the dominant structures recognized in the vicinity of Silver Creek.

The Last Chance is a dip-slip fault with a complex history of reactivation:

1) The north block was UPTHROWN prior to Pennsylvanian time causing the Leadville Limestone to be removed, and the Uncompahgre to be drastically thinned;
2) The north block was DOWNTHROWN during the Pennsylvanian, causing deposition of a thick clastic wedge of lower Hermosa;
3) The south block was UPTHROWN during Laramide doming.

The offset implied during stage 1, the planation of the Uncompahgre Formation, is at least 1,000 meters. The offset during stage 2, implied by the overthickened lower Hermosa Group, is at least 600 meters. This was followed by a period of inactivity along the fault which permitted uniform deposition of the Middle Hermosa carbonates. The last stage of offset is not bracketed in time by lithologic evidence, but probably occurred during the doming associated with widespread intrusion of sills and the Rico monzonite stock in the period 80 to 60 m.y. ago. The Last Chance fault now shows an apparent displacement of about 1,000 meters, north side down, on the Paleozoic-Precambrian unconformity. Baars (1983) suggests that the Last Chance fault is one of a series of Precambrian wrench faults with northwest strikes that localized uplifts from Paleozoic through Laramide time. Baars and Stevenson (1981) also suggest that east-west flexures along these faults localized intrusions. The Last Chance fault bends westward in Silver Creek near the inferred location of the source intrusion, and the Blackhawk fault strikes northwest from the bend. The Blackhawk fault can be traced for about 5 kilometers, but shows only 15 meters of displacement. Both the Last Chance and Blackhawk faults localized near-surface mineralization. The Princeton fault is a pre-mineral, northeast-striking, generally low-angle structure that steepens near its intersection with the Last Chance fault. It may coincide with the sheared Precambrian-Paleozoic unconformity recognized in C-25, C-29, C-30, SC-4, and probably influenced the geometries of the trace element haloes west of the molybdenum deposit.

Mineralization

Mineralization in Silver Creek is elongated

parallel to the Last Chance fault. The contacts between the greenstone and Uncompahgre Formation and between the Uncompahgre and the Hermosa Group also appear to have been important conduits for mineralization. In the four drill holes with thick +0.2% Mo intercepts (SC-1, SC-5, SC-6 & SC-7a), the highest grade intervals occur adjacent to one or both of these contacts (Figures 7 and 8). The best molybdenum intercept (40 meters of 0.5% Mo in drill hole SC-5) overlaps the Uncompahgre/greenstone contact.

Molybdenite and pyrite are the predominate sulfide minerals and occur together in a multi-stage quartz vein stockwork, with minor amounts of scheelite, magnetite, specularite, chalcopyrite, galena, and sphalerite. The minor minerals occur mostly in veins that predate or postdate deposition of the molybdenite. The best tungsten mineralization generally occurs as disseminations within tactites and greenstones, in association with +0.05% Mo. Little or no tungsten mineralization occurs in the Uncompahgre Formation regardless of molybdenum grades.

Homogenization temperatures from 350 to 500°C have been recorded from fluid inclusions in vein quartz associated with molybdenum mineralization. Five liquid-rich and three vapor-rich primary inclusions in drill core from a depth of 784 meters in drill hole C-25 homogenized in the range 362-367°C, and indicate that boiling occurred over that temperature range. Salinities calculated from freezing of the liquid-rich inclusions were consistently less than 1 wt. % NaCl equivalent. The minimum pressure required to maintain boiling of such dilute solutions at 360°C is 184 bars, which implies a depth of formation of 2,000 meters assuming hydrostatic pressure. These data suggest that approximately 1,200 meters of overburden have been eroded from atop the deposit in the 5 million years since mineralization formed.

Wall-Rock Alteration

Alteration zoning (Figures 9 and 10) around the molybdenum deposit is controlled by the original hostrock compositions and distance from the source intrusion. Alteration in non-calcareous rocks ranges from a potassic core to distal phyllic and propylitic assemblages. In calcareous rocks, garnetization grades outward into an anhydrite-diopside assemblage.

The potassic alteration assemblage is orthoclase, biotite and sericite with minor chlorite, anhydrite, and epidote. Potassic alteration is always associated with a quartz vein stockwork. The siltstones and greenstone are hornfelsed and bleached in the potassic zone, whereas the arkose and quartzite are not significantly altered. Most of the +0.2% Mo mineralization occurs within the potassic zone.

The phyllic zone lies above the potassic zone and is characterized by an assemblage of sericite, biotite, chlorite, and minor orthoclase. Sphene and chlorite replace primary mafic minerals in the hornblende latite porphyry, whereas secondary sericite, chlorite, and/or biotite are present in the arkoses. Siltstones and the greenstone are bleached and somewhat hornfelsed. Phyllic alteration is present as narrow haloes around the major structures in the Blaine mine and for several thousand meters to the west along the Last Chance fault. The boundary between the potassic zone and the phyllic zone is gradational and corresponds to a decrease in quartz veining near the 0.05% Mo grade contour. The upper phyllic zone boundary coincides with the disappearance of pervasive quartz veining.

Propylitic alteration is recognized in near-surface arkoses and intrusions, and is characterized by partial sericitization of feldspars and replacement of mafic minerals by chlorite and epidote.

The garnet zone is confined to the basal 100 meters of the Hermosa section. It contains most of the tungsten mineralization and locally includes +0.2% Mo.

The anhydrite-diopside zone extends above the garnet zone approximately 250 meters, and consists of interbedded massive diopside that has replaced silty carbonate units and massive anhydrite that has replaced limestones.

Magnetite and orthoclase occur within quartz-molybdenite veins and vein selvages at the base of the garnet zone. Vein selvages in the upper garnet and anhydrite-diopside zones comprise biotite that grades both laterally and distally to actinolite.

Anhydrite veins occur within the Precambrian rocks but are more abundant in the Hermosa sediments. They commonly contain specularite and minor base metal sulfides, and are paragenetically younger than both the massive anhydrite and the quartz-molybdenite veins.

The origin of the sulfate in the anhydrite replacements is controversial. The Hermosa Group west of Rico includes the Paradox Formation, a sequence of interbedded limestones and evaporites. Similar evaporites have not been recognized in the immediate Rico area, but may have existed in the section that was massively garnetized. Replacement of limestones above the garnet zone may have required only minor remobilization of syngenetic anhydrite. Carbon dioxide bubbles observed in fluid inclusions in the massive anhydrite suggest that substantial pressure corrections are required on homogenization temperatures that range from 75-150°C. The carbon dioxide probably evolved by hydrothermal alteration of calcite to anhydrite (Reynolds, 1981).

Geochemistry

Pervasive dispersion haloes of molybdenum, tungsten and fluorine occur above the Silver Creek deposit, and are especially well-developed and extensive in the Hermosa Group north of the Last Chance fault. Tin, thallium, rubidium, strontium and niobium show sporadic anomalies.

Molybdenum increases gradually with depth to within a few hundred meters of +0.2% Mo where a very rapid increase is observed (Figures 7 and 8). Near-surface samples very rarely exceed 1 ppm except along major structures.

Tungsten forms a relatively tight halo immediately above the 0.2% Mo contour, where it coincides with the occurrence of the lowest

calcareous part of the Hermosa. Scheelite and powellite are the principal tungsten minerals.

Fluorine forms the most extensive trace element halo and increases steadily from about 1,000 ppm at the surface to several percent at the upper 0.2% Mo grade contour. Sericite is inferred to contain most of the anomalous fluorine, because only traces of fluorite have been identified in the Silver Creek area.

The drilled portion of the Silver Creek deposit lies beneath the Blaine mine, at the intersection of the Last Chance and Blackhawk faults. These faults are exposed in the workings of the Blaine mine as locally gougy quartz and calcite veins that are strongly anomalous in tungsten, fluorine and molybdenum. Sampling of the faults both underground and at the surface yielded information that helped locate the deposit.

Phyllic alteration, in association with lenses of pyrite and magnetite, projects nearly to the surface adjacent to the major structures. Lead-zinc-silver, and copper-iron mineralization associated with the Silver Creek deposit occurs peripheral to the phyllic haloes above an elevation of 2,400 meters, and extends several thousand meters laterally from the surface projection of the molybdenum resource.

Conclusions

The Silver Creek molybdenum deposit at Rico, Colorado was discovered by persistent, aggressive explorationists and managers during an economic environment conducive to high-risk exploration. The application of the Climax-type molybdenum exploration model was essential to the discovery, and fluorine, tungsten and molybdenum gradients were key elements used to direct the exploration drilling program.

Although the Silver Creek deposit has been only partially tested by drilling, it appears to be very large and very high grade. Approximately 44 million tons of 0.31% Mo have been indicated by drilling, using a 0.2% Mo cutoff. Two factors suggest that the grade may be increased by additional drilling; 1)the geologic center (source intrusion) of the deposit has not been located; and 2)the structural control of the Last Chance fault suggests that a high grade keel may occur in an untested area where the fault intersects the mineralized zone. The top of the known deposit is 1,200 meters below the Blaine adit at an elevation of 1,615 meters, and the deepest known extent is 1,380 meters elevation, a vertical range of 235 meters. The width of the drilled deposit is approximately 580 meters, and the length remains unknown. Projections of the outline of +0.2% Mo indicate that the deposit may exceed 200 million tons.

Acknowledgements

The authors have drawn on significant contributions by Anaconda geologists: J. Bielak, R. Casaceli, G. Dimo, P. Larsen, M. Little, J. Rushing, D. Silver and W.A. Wright. Each one of these people contributed to the success of this project.

Special recognition goes to W. J. Garmoe wholed Anaconda into the Rico Project, to J. R. King who first identified the potential for a porphyry molybdenum target in the Silver Creek area, and to Orval Jahnke for sharing his long-term knowledge of the Rico district.

References

Baars, D. L., 1983, "San Luis Uplift -- Fact or Fiction," Geol. Soc. Am. Abst. with Programs, v. 15, no. 5, p. 392.

Baars, D. L. and Stevenson, G. M., 1981, "Tectonic Evolution of the Paradox Basin," in Geology of the Paradox Basin: Rocky Mtn. Assoc. Geol. 1981 Field Conf., p. 2082-2111.

McKnight, E. T., 1974, "Geology and Ore Deposits of the Rico District, Colorado," U.S.G.S. Pro. Paper 723, p. 1-100.

Naeser, C. W., Cunningham, C. G., Marvin, R. F., and Obradovich, J. D., 1979, "Pliocene Intrusive Rocks and Mineralization Near Rico, Colorado," U.S.G.S. Open-File Report 79-1093, p. 1-19.

Ranta, D. E., White, W. H., Ward, A. D., Graichen, R. E., Ganster, M. W., and Stewart, D. R., 1976, "Geology of the Urad and Henderson Molybdenite Deposits -- A Review," in Epis, R. C. and Weimer, R. J., eds., no. 8, p. 477-485.

Reynolds, T. J., 1981, "Fluid Inclusion Study of Massive Anhydrite from the Silver Creek Prospect, Rico, Colorado," Unpublished Anaconda report.

Rushing, J. A., 1979, "Geologic Map of the Rico District," Unpublished Anaconda data.

Wallace, S. R., MacKenzie, W. B., Blair, R. G., and Muncaster, N. K., 1978, "Geology of the Urad and Henderson Molybdenite Deposits, Clear Creek County, Colorado, with a Section on a Comparison of These Deposits with Those at Climax, Colorado," Econ. Geol., v. 73, no. 3, p. 325-368.

Table 1. Analysis of Silicic Alkali-Alaskite

Oxide	Wt. %
SiO_2	78.50
TiO_2	0.10
Al_2O_3	11.00
Fe_2O_3	0.70
FeO	--
MnO	0.01
MgO	0.20
CaO	0.65
Na_2O	2.20
K_2O	5.10
P_2O5	0.12
	98.58

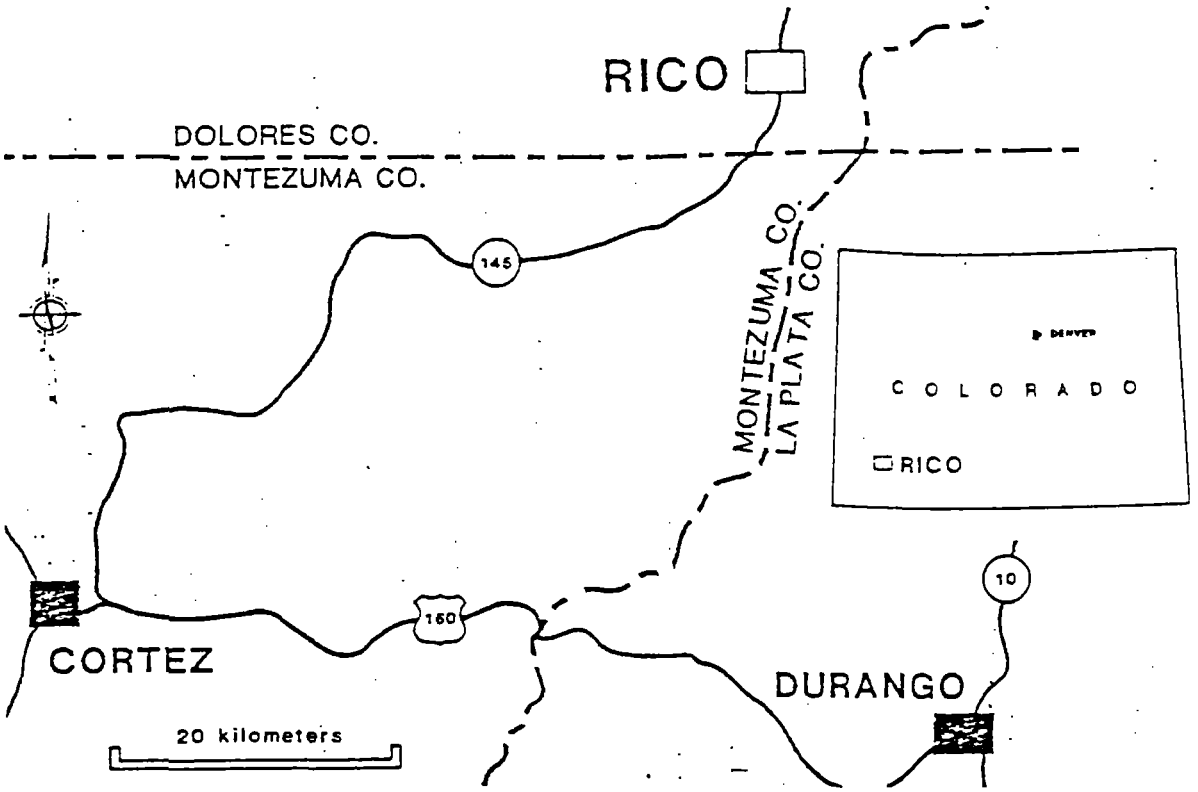

Figure 1. Location of the Rico mining district.

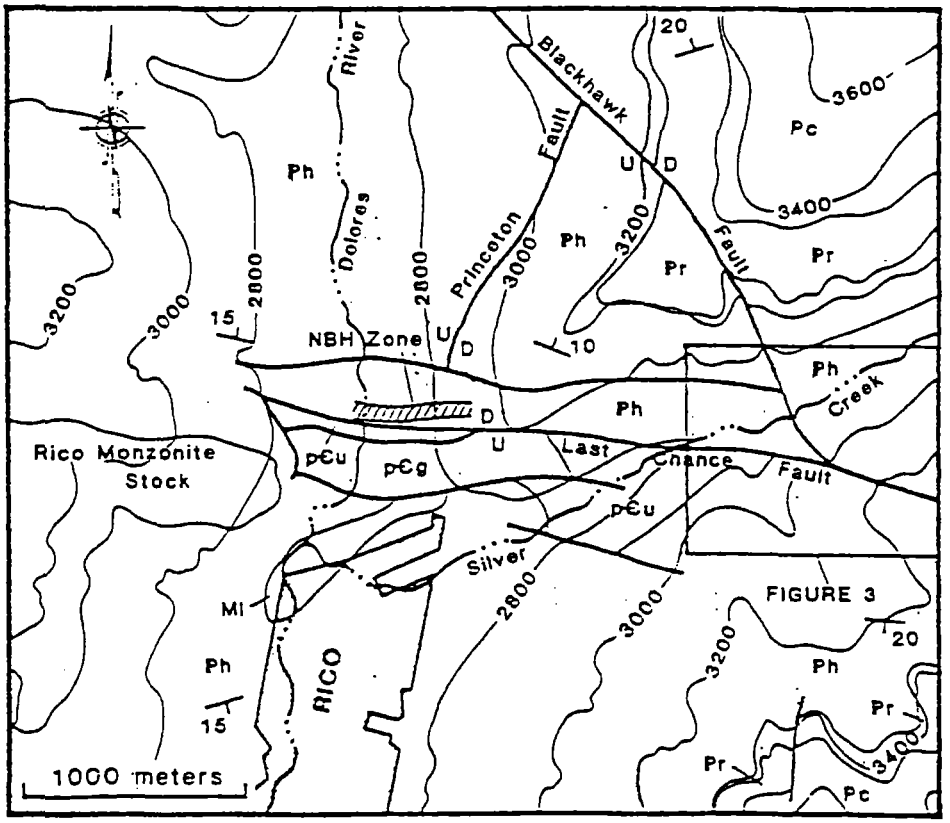

Figure 2. Rico district geology.

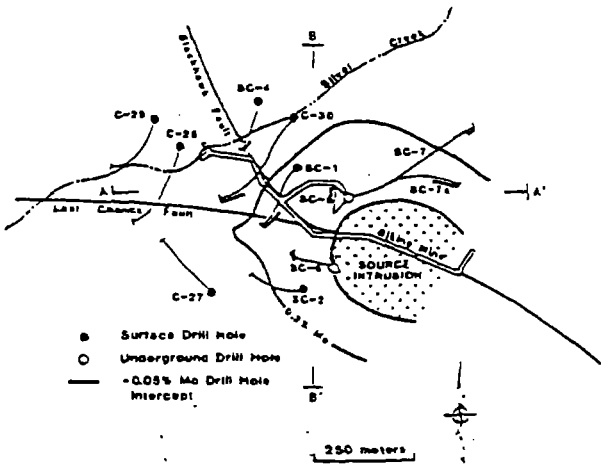

Figure 3. Silver Creek area drill hole location map.

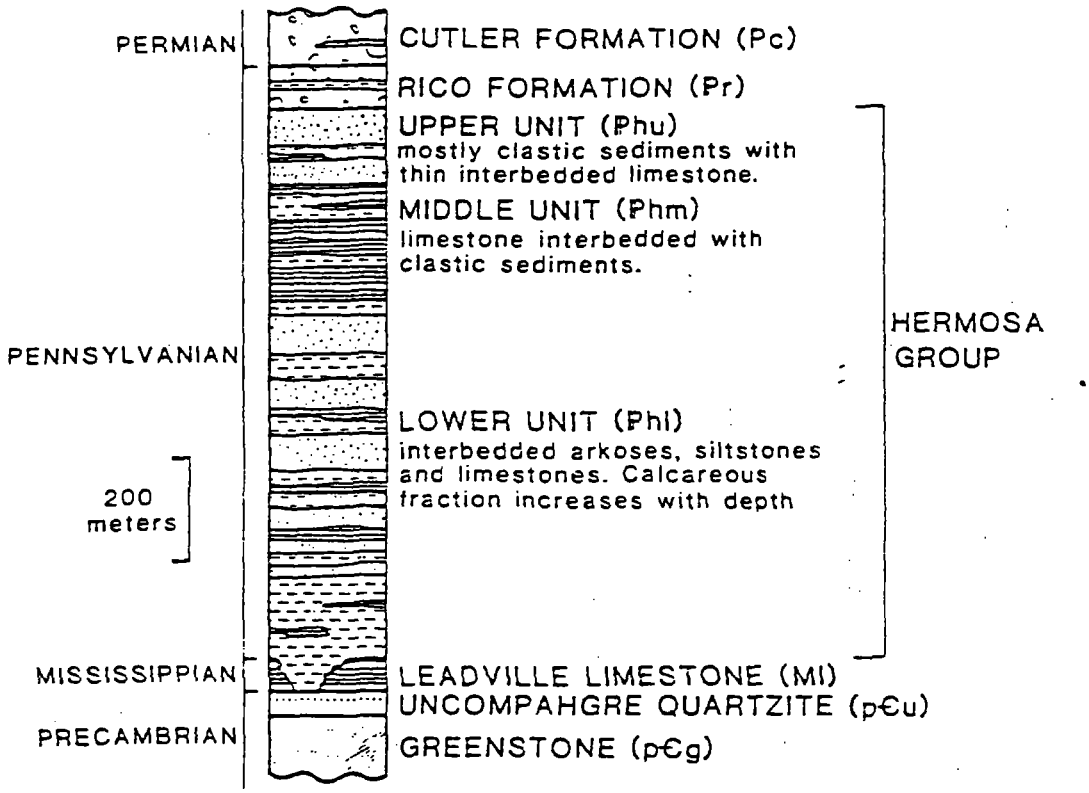

Figure 4. Stratigraphic column for the Rico district.

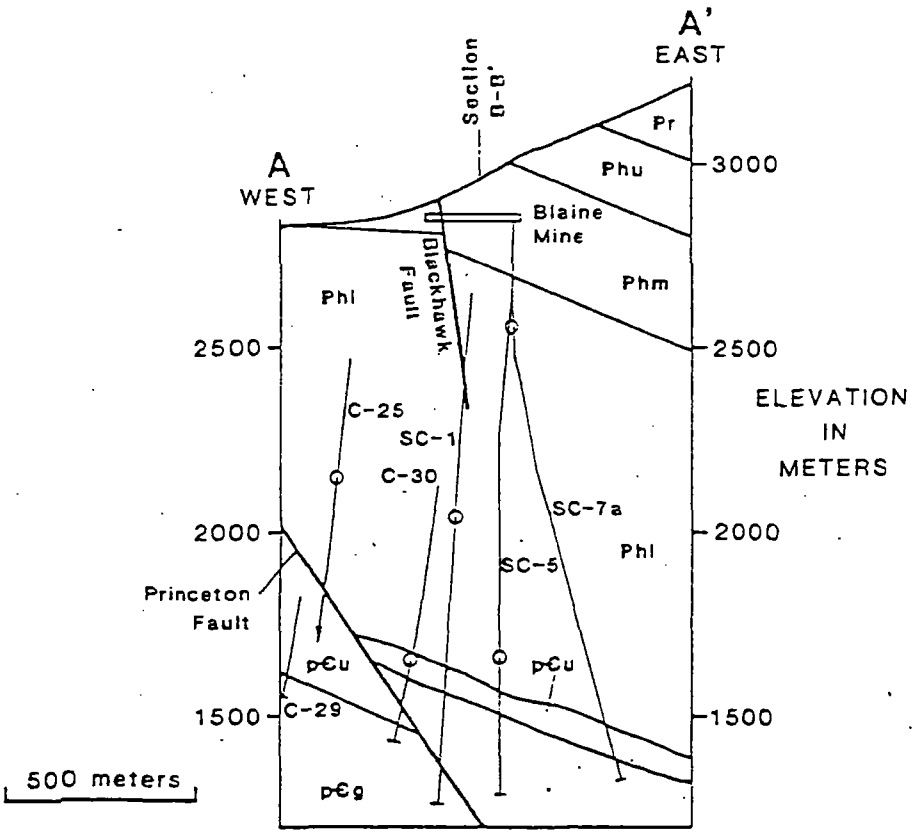

Figure 5. East-west geologic section of Silver Creek area.

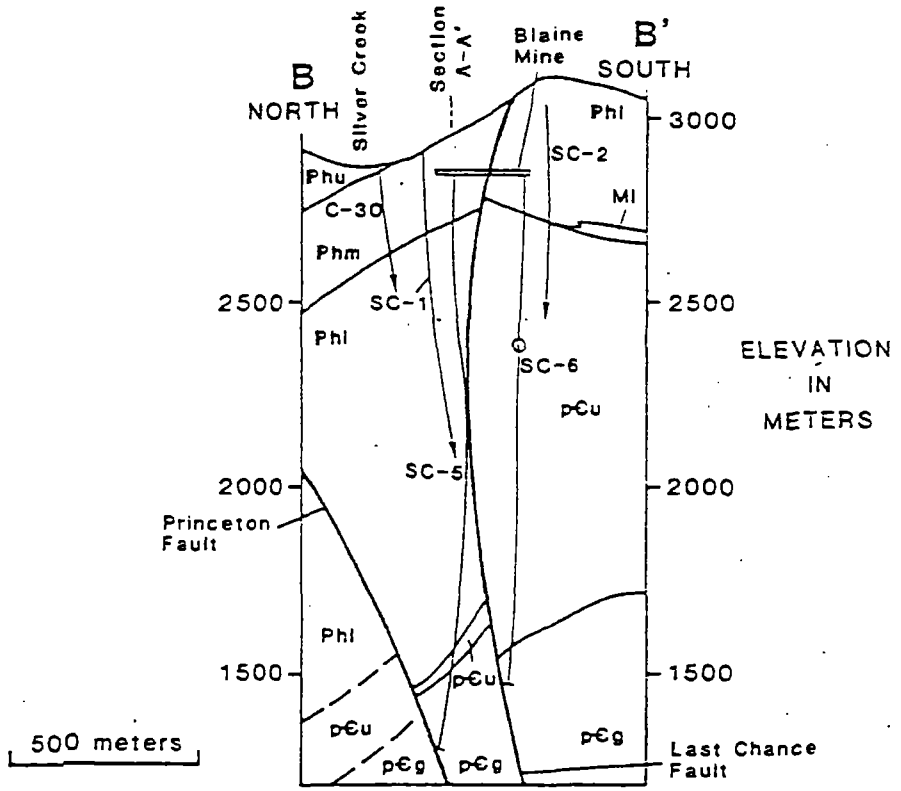

Figure 6. North-south geologic section of Silver Creek area.

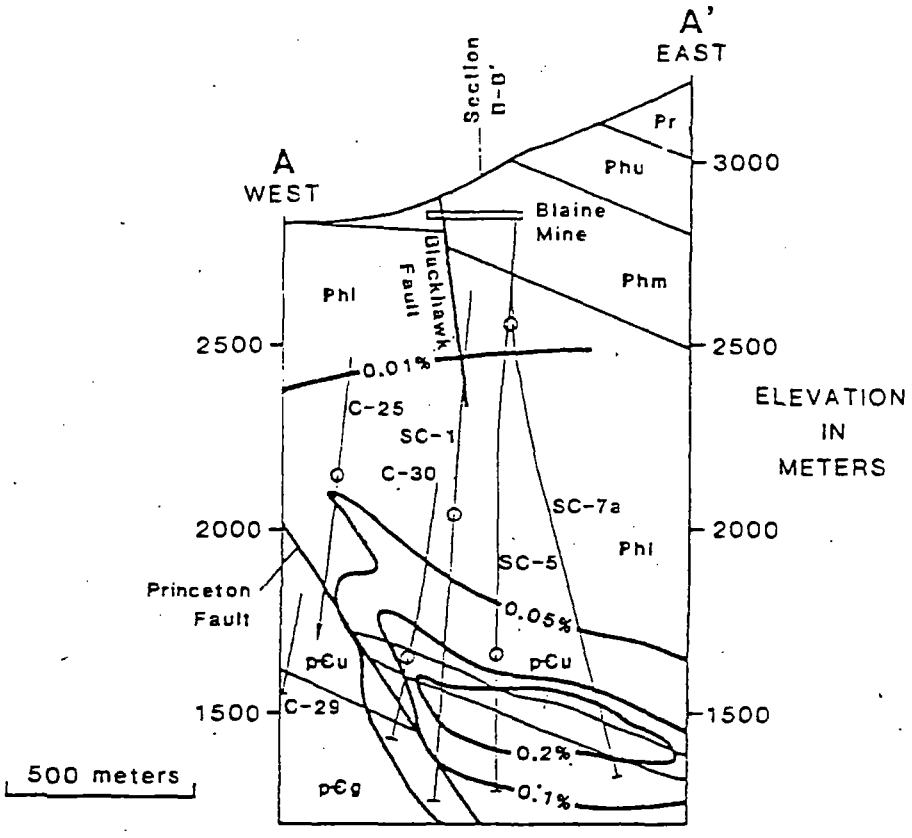

Figure 7. East-west section of Silver Creek area showing molybdenum grades.

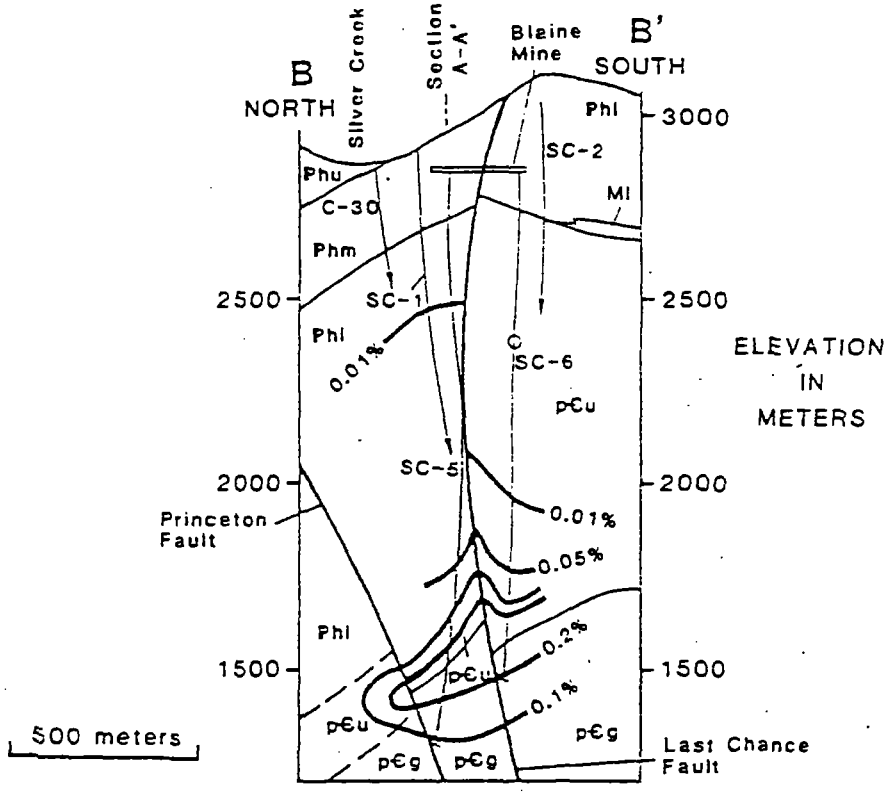

Figure 8. North-south section of Silver Creek area showing molybdenum grades.

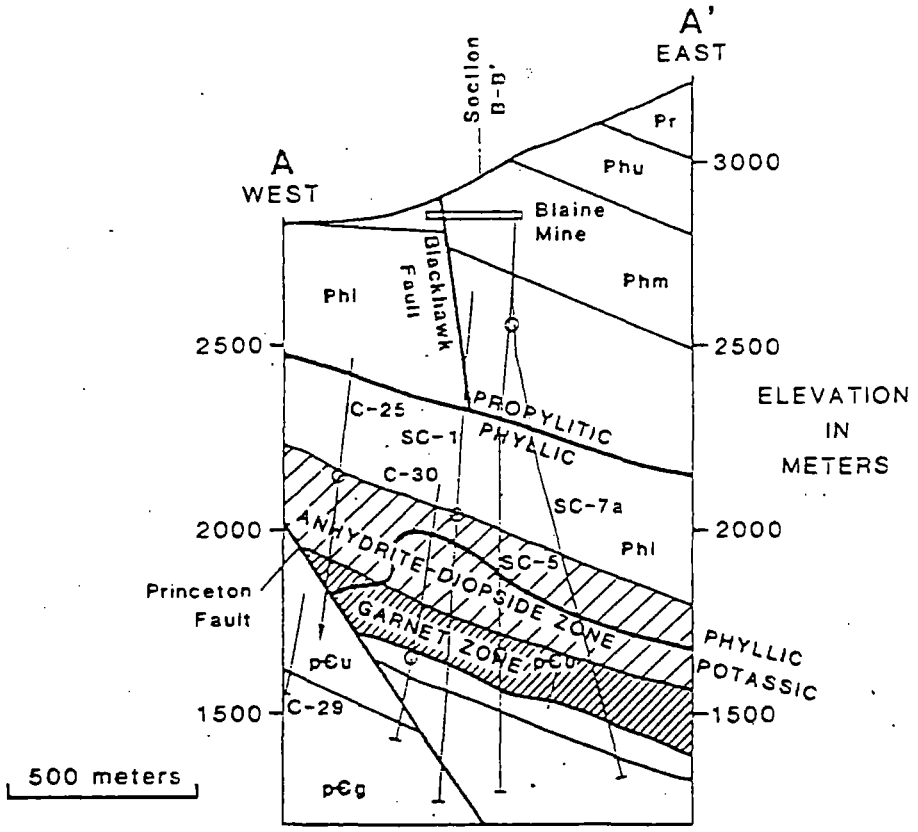

Figure 9. East-west section of Silver Creek area showing alteration zones.

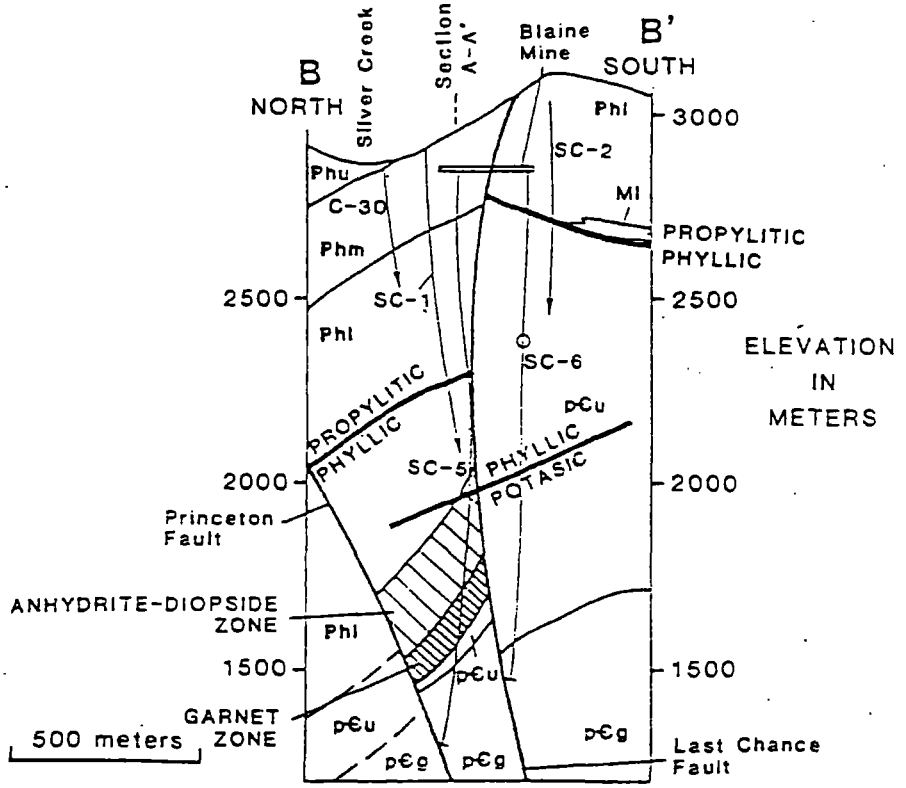

Figure 10. North-south section of Silver Creek area showing alteration zones.

Economic Geology
Vol. 75, 1980, pp. 122–133

SCIENTIFIC COMMUNICATIONS

PLIOCENE INTRUSIVE ROCKS AND MINERALIZATION NEAR RICO, COLORADO

Fission-track and potassium-argon studies of intrusive rocks in the vicinity of Rico, Colorado, have shown that there are at least two periods of igneous activity and that significant ore mineralization is associated with alaskites and latites that are 3 to 5 m.y. old. Discordant fission track ages of apatite and zircon in the older rocks reveal a major heat source that cooled in late Miocene or early Pliocene and is centered under the mineralized rocks near the townsite of Rico. This heating may indicate the presence of a buried stock that is related to the mineralization.

Introduction and Geologic Setting

Rico, Colorado, is a precious and base metal mining camp situated on the Dolores River in the western San Juan Mountains. Previous reports on the geology and mineralization include Farish, 1892; Rickard, 1897; Cross and Spencer, 1900; Ransome, 1901; Cross and Ransome, 1905; Pratt, 1968; Pratt et al., 1969; and McKnight, 1974.

Rico is near the center of the Rico dome, which is a major east-west-trending, breached, elliptical dome with a long axis of about 5 km. The dome consists of uplifted Mississippian to Cretaceous sedimentary rocks around a core containing a horst of Precambrian rocks that have been uplifted more than 2 km. Detailed stratigraphic sections are given in McKnight, 1974.

Geochronologic Methods

Twelve intrusive rocks and one sericite from a vein were dated as part of this study. Table 1 shows 21 fission-track ages on apatite, zircon, and sphene concentrates. Table 2 lists two K-Ar ages, one biotite age, and one sericite age. The map (Fig. 1) shows the location and ages of all samples dated in this study.

The fission track ages were determined using the procedures outlined in Naeser (1976). The zircon and sphene were dated using the external detector method, and the population method was used for dating the apatite. The standard error of the zircon and sphene ages was calculated using the procedure outlined by Naeser et al. (1978). The errors on the apatite ages were calculated by combining the Poisson errors on the fossil and induced counts (Lindsey et al., 1975). The neutron doses were determined by using National Bureau of Standards glass SRM962. The neutron doses were calibrated against the NBS copper neutron dose.

Intrusive Rocks and Age Relationships

Igneous rocks have been emplaced during at least two episodes. Cretaceous?-Paleocene hornblende latite rocks intrude the sedimentary rocks. The hornblende latites are generally present as sills, but at least one large discordant body cuts sedimentary rocks several kilometers east of Rico, near Hermosa Peak (Pratt, 1976). This body has a minimum age of 57.2 ± 6.9 m.y. (fission track, zircon) and older ages of 80.1 ± 2.4 m.y. (K-Ar, hornblende) and 78 ± 16 m.y. (fission track, sphene) (Marvin et al., 1974, No. 137). Armstrong (1969) reported an age on hornblende latite collected several kilometers south of Rico as 179 m.y. for a pyroxene concentrate and 61.3 m.y. for the whole rock with the heavy minerals removed. Preliminary studies of the rocks in the Colorado mineral belt (Cunningham et al., 1977) provided ages on the hornblende latite of 65 m.y. (fission track, zircon) and 20.2 m.y. (fission track, apatite), indicating that the rock had been partly thermally reset. Ages of zircons from three samples collected for this study range from 59.9 ± 2.7 to 64.9 ± 3.7 m.y., indicating that the rock formed close in time to the Mesozoic-Tertiary boundary.

A second major Cretaceous?-Paleocene rock type is augite monzonite, which forms a composite stock west of Rico. Pratt et al. (1969) indicated that the augite monzonite intrudes the hornblende latite; McKnight (1974, p. 42) believed they were nearly contemporaneous; and our studies show sphene from the augite monzonite as 78 m.y. old, indicating that it may be the oldest rock, although definitive field relationships are lacking. The augite monzonite has been thermally reset, and discordant ages ranging from 82 m.y. (K-Ar, hornblende) Marvin et al., 1974, No. 132) to 6.6 ± 2.3 m.y. (fission track, apatite) have been determined. The hornblende latite and augite monzonite compose most of the igneous rock exposed at the surface.

TABLE 1. Fission-Track Ages, Rico, Colorado

Sample	Mineral	Number of grains	r[1], $\bar{s}_i$[2]	ρs 10^6 tracks/cm²	ρi 10^6 tracks/cm²	ϕ 10^{15} n/cm²	U ppm	Age ± 2σ 10^6 yr
Augite monzonite								
Rico 1	Sphene	6	0.99 (r)	8.46 (1645)[3]	12.15 (1181)[3]	1.89	210	78.4 ± 3.3
	Zircon	6	0.98 (r)	4.78 (1174)	4.86 (596)	1.04	150	61.4 ± 2.9
	Apatite	50	0.068 ($\bar{s}_i$)	0.016 (34)	0.169 (353)	1.14	4.8	6.6 ± 2.3
Hornblende latite-porphyry								
Rico 2	Zircon	6	0.99 (r)	9.89 (2151)	9.72 (1058)	1.07	290	64.9 ± 2.9
	Apatite	50	0.115 ($\bar{s}_i$)	0.017 (36)	0.038 (121)	1.14	1.6	20.2 ± 7.4
Rico 3	Zircon	6	0.78 (r)	11.77 (1835)	10.75 (838)	0.996	310	64.9 ± 3.7
	Apatite	50	0.099 ($\bar{s}_i$)	0.010 (29)	0.058 (162)	0.961	1.7	10.3 ± 4.1
Rico 4	Zircon	6	0.94 (r)	6.12 (850)	10.58 (735)	0.994	310	34.3 ± 1.5
	Apatite	50	0.125 ($\bar{s}_i$)	0.004 (11)	0.049 (137)	0.961	1.5	4.6 ± 2.9
Rico 5	Zircon	6	0.84 (r)	1.29 (219)	11.29 (957)	0.991	330	6.8 ± 0.6
	Apatite	50	0.159 ($\bar{s}_i$)	0.007 (20)	0.059 (165)	0.961	1.8	7.0 ± 3.3
Rico 6	Zircon	6	0.96 (r)	10.74 (1856)	10.56 (913)	0.989	310	59.9 ± 2.7
	Apatite	50	0.10 ($\bar{s}_i$)	0.007 (20)	0.053 (148)	0.961	1.6	7.8 ± 3.7
Rico 9	Zircon	6	0.98 (r)	9.74 (1650)	14.82 (1256)	0.986	430	38.6 ± 1.5
	Apatite	50	0.10 ($\bar{s}_i$)	0.005 (14)	0.051 (143)	0.961	1.5	5.6 ± 3.2
Calico Peak porphyry								
Rico 10 (stock)	Zircon	6	0.86 (r)	1.45 (271)	21.04 (1961)	0.984	620	4.1 ± 0.4
Rico 11 (dike)	Zircon	6	0.99 (r)	0.865 (170)	9.00 (885)	0.982	260	5.6 ± 0.5
Rico 14 (sill)	Zircon	6	0.92 (r)	0.931 (221)	13.42 (1592)	0.975	400	4.0 ± 0.4
	Apatite	50	0.05 ($\bar{s}_i$)	0.027 (77)	0.258 (725)	0.961	7.7	6.1 ± 1.5
Alaskite porphyry								
Rico 12	Zircon	6	0.93 (r)	1.12 (209)	19.60 (1827)	0.979	580	3.4 ± 0.3
Rico 13	Zircon	6	0.99 (r)	1.08 (147)	16.21 (1099)	0.977	480	3.9 ± 0.4

[1] Correlation coefficient.
[2] Standard error of mean induced tracks.
[3] ( )Number of tracks counted.
$\lambda_F = 7.03 \times 10^{-17}$ yr^{-1}.

The older rocks of the Rico dome are intruded by dikes that include augite lamprophyre, hornblende lamprophyre, basalt, alaskite porphyry, and porphyritic augite latite. We have dated the alaskite porphyry as Pliocene, but the absolute ages of the other dikes are unknown. Pratt et al. (1969) reported that augite lamprophyre and basalt dikes cut the hornblende latite.

A stock and several dikes, collectively called the Calico Peak Porphyry (Pratt et al., 1969), were intruded 4.6 ± 0.5 m.y. ago (average of three zircon fission-track ages). The largest intrusive is a stock that cuts sedimentary rocks at Calico Peak. The rock is a biotite-hornblende latite that is pervasively altered. A similar rock type that is much less altered forms a sill several kilometers south of Calico Peak near Priest Gulch. It has a K-Ar age of 4.5 ± 0.2 m.y. (biotite).

A distinctive alaskite porphyry forms several dikes near the town of Rico and is associated with significant mineralization. Zircon from two samples of this dike were dated. Sample 12 from Aztec Gulch, west of Rico, has an age of 3.4 ± 0.3 m.y.; and sample 13 from along Silver Creek, east of town, has an age of 3.9 ± 0.4 m.y. This is the youngest rock we have dated in the area. It may also be the youngest rhyolite in the San Juan volcanic field; the youngest one that Lipman et al. (1978) reported is dated at 4.8 m.y. The basalt dikes and alaskite dikes are probably essentially contemporaneous and part of the bimodal suite recognized by Lipman et al. (1970).

Thermal Overprint

A thermal event reset the ages of apatites in all of the older rocks . The one sample we dated of the

TABLE 2. K-Ar Ages, Rico, Colorado

Sample	Mineral	K_2O (percent)	Radiogenic ^{40}Ar (10^{-10} mol/g)	Radiogenic ^{40}Ar (percent)	Age (m.y.) ±2σ
Calico Peak Porphyry					
Rico 14 (sill)	Biotite[1]	8.50 8.53	0.5479	43	4.5 ± 0.2
Vein along Black Hawk fault[2]					
57-491	Sericite[3]	8.44	0.799	64.3	5.45 ± 0.2
57-491I	Sericite[3]	8.34	0.780	56.8	5.39 ± 0.2

[1] Analysts: R. F. Marvin, H. H. Mehnert, and V. M. Merritt.
[2] Analyst: J. D. Obradovich.
[3] Sericite from near intersection of Argentine tunnel and Black Hawk fault (McKnight, 1974).
Constants: $K^{40}\lambda_\epsilon = 0.581 \times 10^{-10}$/yr; $\lambda_\beta = 4.962 \times 10^{-10}$/yr; $K^{40}/K = 1.67 \times 10^{-4}$ atomic ratio.

Base map U.S. Geological Survey, 1960

Geology modified from Pratt, McKnight, and De Hon, 1969

FIG. 1. Simplified geologic map of the Rico quadrangle, Colorado.

Description of Map Units

Qs = surficial deposits (Quaternary)—includes alluvium, fan deposits, talus, slopewash, landslide deposits, and calcareous tufa.

Tap = alaskite porphyry dikes (Pliocene)—light gray to white rhyolite containing partly resorbed quartz phenocrysts in an aphanitic groundmass of K-feldspar and quartz.

Tcl = Calico Peak Porphyry (Pliocene)—porphyritic biotite-hornblende latite; brownish-gray rock containing phenocrysts of sanidine, plagioclase, hornblende, and biotite in an aphanitic groundmass of quartz and feldspar; contains minor Fe-Ti oxides, apatite, sphene and zircon.

Tca = Calico Peak Porphyry (Pliocene)—altered porphyritic biotite-hornblende latite; light gray to light brown porphyritic rock containing phenocrysts of plagioclase and K-feldspar in an altered aphanitic groundmass; alteration minerals include alunite and sericite.

Td = Dikes (Pliocene?)—dikes of varying lithologies, including augite lamporphyre, hornblende lamprophyre, basalt, and porphyritic augite latite.

TKhl = hornblende latite-porphyry (Paleocene to Cretaceous?)—light to dark gray, porphyritic latite containing phenocrysts of andesine and hornblende in an aphanitic groundmass of plagioclase, orthoclase, minor quartz, Fe-Ti oxides, apatite, and zircon; rock is pervasively propylitized and locally sericitized.

TKm = augite monzonite (Paleocene to Cretaceous?)—gray, hypidiomorphic granular monzonite containing andesine, interstitial orthoclase, green augite ± hornblende ± biotite, conspicuous sphene, minor quartz, zircon, and apatite.

KMs = sedimentary rocks (Cretaceous to Mississippian)—includes Dakota Sandstone, Morrison Formation, Wanakah Formation, Entrada Sandstone, Dolores Formation, Cutler Formation, Rico Formation, Hermsa Formation, quartzite of Larsen tunnel area, and Leadville Limestone.

p∈ = Uncompahgre Quartzite, Metadiorite, and Greenstone (Precambrian).

Contact, degree of certainty not indicated; fault, dashed where inferred, dotted where concealed, bar and ball on downthrown side; approximate crestline of elongated dome.

1 = sample number, Tables 1 and 2; A = apatite fission-track age; Z = zircon fission-track age; S = sphene fission-track age; B = biotite K-Ar age.

Correlation of map units

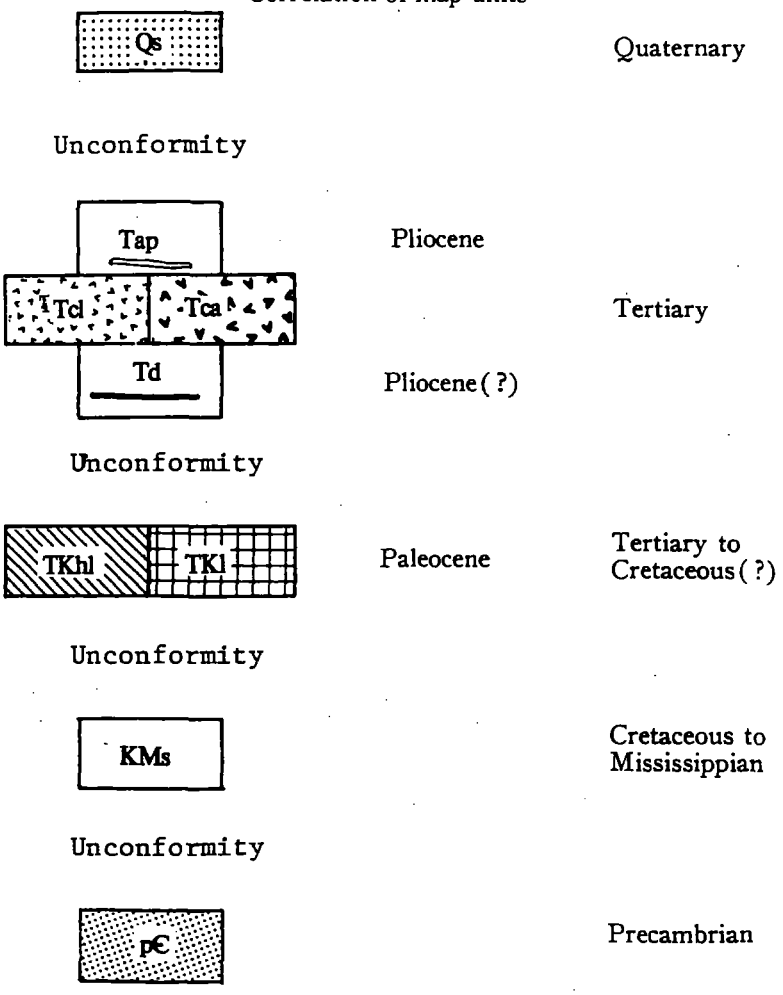

augite monzonite (1)* has a zircon age of 61.4 ± 2.9 m.y. and an apatite age of 6.6 ± 2.3 m.y. The apatite ages on the hornblende latite-porphyry are all much younger than the intrusive ages of the porphyry and range from 20.2 ± 7.4 m.y. (2) in the southern part of the district to 4.6 ± 2.9 m.y. (4) near the center of the district. Three samples of the hornblende latite from within the mining district were dated. The zircon ages from these samples have all been lowered. They range from 38.6 ± 1.5 m.y. (9) to 6.8 ± 0.6 m.y. (5). The hornblende and sphene are systematically older than the biotite and zircon, suggesting that the biotite and zircon are partly reset.

The annealing of fission tracks in minerals is known to take place at temperatures as low as 100°C (Naeser, 1979). Apatite will suffer track loss at temperatures between 90° and 150°C over periods of time lasting 10^5 years or longer (Naeser and Faul, 1969). The track annealing in zircon is less well known; Naeser has estimated that it occurs at temperatures between 175° and 225°C. Track loss is a gradational process, and partial track loss is possible. This is seen by the apatite ages from samples 2 and 3 and the zircons from samples 1, 4, and 9. Total annealing of apatite was observed in samples 1, 4, 5, 6, and 9. These five apatites have an average age of 6.3 ± 0.6 m.y., and therefore must have cooled from a temperature in excess of 130°C about 6 m.y. ago. One sample (5) was heated in excess of 200°C. The zircon from that sample has an age of 6.8 ± 0.6 m.y., which is concordant with the age of the apatite.

The pattern of reduced fission-track ages on apatite and zircon delineated in this report points to a major thermal disturbance in the Rico area. This disturbance is probably centered near the location of sample 5. We postulate that a stock, probably related to the Calico Peak Porphyry or the alaskite porphyry, is present at depth just east of Rico.

Mineralization

The Rico mining district has produced gold, silver, copper, lead, and zinc intermittently since 1879. The known deposits consist of sulfide replacement deposits and contact-metamorphic deposits in limestones and veins in clastic rocks (McKnight, 1974).

The ages of all of the mineralization and the relationships to rock units are poorly known. Rickard (1897) observed that the ore veins penetrated the porphyry (apparently the hornblende latite-porphyry) in the ore deposits on Newman Hill, immediately southeast of Rico. The literature does not contain any reference to genetic relationships between the alaskite porphyry and sulfide ore. Both samples of alaskite porphyry collected for this study are altered, and sample 12 contains disseminated sulfides and is cut by small sulfide-bearing veins. This suggests that the alaskite porphyry may be genetically related to some, if not all, of the ore. This is further supported by the single sample of sericite from the ore vein along the Black Hawk fault, which has a K-Ar age of about 5.5 m.y. The coincidence in time and space between the young mineralization, young intrusive rocks, and hidden thermal center east of Rico suggests that this may be the site for a young, unexposed stock with the potential for porphyry-type mineralization.

The axis of the Rico dome is the loci of the augite monzonite stock and possibly governs the location of a hidden stock. The horst of Precambrian rock may be related to the intrusion of this hidden pluton. The relationship between superimposed centers of intrusion and mineralization has been well documented at Climax and Henderson (Wallace et al., 1968, 1978).

Another potential source of economic mineralization is the Calico Peak Porphyry stock at Calico Peak. The alteration assemblage includes significant quantities of alunite. Experimental evidence (Hemley et al., 1969) has shown that, to form alunite in this environment, sulfur and a hydrothermal system are needed—two ingredients conducive to ore formation. Alteration features at Calico Peak are similar to the alteration features at Marysvale, Utah, where Cunningham et al. (1978) have shown a time-space genetic relationship between alunite alteration and the precious to base metal mineralization, and have predicted the presence of a hidden porphyry deposit. Sulfides, tentatively identified as molybdenite, have been reported from the Calico Peak Porphyry (W. P. Pratt, oral commun., 1979).

Acknowledgments

We thank Walden P. Pratt and Harald H. Mehnert for their helpful reviews, Ezekiel Rivera for his help with mineral separations, and Gail A. Wadsworth, Lori B. Glassgold, and Richard E. Schoenfeld for their help with the drafting.

C. W. Naeser
C. G. Cunningham
R. F. Marvin
J. D. Obradovich

U. S. Geological Survey
Denver, Colorado 80225
June 20, 1979; August 20, 1979

* The numbers in parentheses refer to sample localities in Figure 1.

REFERENCES

Armstrong, R. L., 1969, K-Ar dating of laccolithic centers of the Colorado plateau and vicinity: Geol. Soc. America Bull., v. 80, p. 2081–2086.

Cross, Whitman, and Ransome, F. L., 1905, Description of the Rico quadrangle [Colorado]: U. S. Geol. Survey Geol. Atlas, Folio 130, 20 p.

Cross, Whitman, and Spencer, A. C., 1900, Geology of the Rico Mountains, Colorado: U. S. Geol. Survey, 21st Ann. Rept., pt. 2, p. 7–165.

Cunningham, C. G., Naeser, C. W., and Marvin, R. F., 1977, New ages for intrusive rocks in the Colorado mineral belt: U. S. Geol. Survey Open-File Rept. 77–573, 7 p.

Cunningham, C. G., Steven, T. A., and Naeser, C W., 1978, Preliminary structural and mineralogical analysis of the Deer Trail Mountain-Alunite Ridge mining area, Utah: U. S. Geol. Survey Open-File Rept. 78–314.

Farish, J. B., 1892, On the ore deposits of Newman Hill, near Rico, Colorado: Colorado Sci. Soc. Proc., v. 4, p. 151–164.

Hemley, J. J., Hostetler, P. B., Gude, A. J., and Mountjoy, W. T., 1969, Some stability relations of alunite: Econ. Geol., v. 64, p. 599–612.

Lindsey, D. A., Naeser, C. W., and Shawe, D. R., 1975, Age of volcanism, intrusion, and mineralization in the Thomas Range, Keg Mountain, and Desert Mountain, western Utah: U. S. Geol. Survey, Jour. Research, v. 3, p. 597–604.

Lipman, P. W., Steven, T. A., and Mehnert, H. H., 1970, Volcanic history of the San Juan Mountains, Colorado, as indicated by potassium-argon dating: Geol. Soc. America Bull., v. 81, p. 2329–2352.

Lipman, P. W., Doe, B. R., Hedge, C. E., and Steven, T. A., 1978, Petrologic evolution of the San Juan volcanic field, southwestern Colorado: Pb and Sr isotope evidence: Geol. Soc. America Bull., v. 89, p. 59–82.

Marvin, R. F., Young, E. J., Mehnert, H. H., and Naeser, C. W., 1974, Summary of radiometric age determinations on Mesozoic and Cenozoic igneous rocks and uranium and base metal deposits in Colorado: Isochron West, no. 11, p. 1–41.

McKnight, E. T., 1974, Geology and ore deposits of the Rico district, Colorado: U. S. Geol. Survey Prof. Paper 723, 100 p.

Naeser, C. W., 1976, Fission track dating: U. S. Geol. Survey Open-File Rept. 76–190, 68 p.

—— 1979, Fission-track dating and geologic annealing of fission tracks, *in* Jager, E., and Hunziker, J., eds., Lectures in isotope geology: Heidelberg, Springer-Verlag, p. 154–169.

Naeser, C. W., and Faul, H., 1969, Fission track annealing in apatite and sphene: Jour. Geophys. Research, v. 74, p. 705.

Naeser, C. W., Johnson, N. M., and McGee, V. E., 1978, A practical method of estimating standard error of age in the fission-track dating method: U. S. Geol. Survey Open-File Rept. 78–701, p. 303–304.

Pratt, W. P., 1968, Summary of the geology of the Rico region, Colorado, *in* New Mexico Geological Society Guidebook, 19th Field Conference, San Juan-Miguel-La-Plata region, New Mexico and Colorado, 1968: New Mexico Bur. Mines Mineral Resources, p. 83–87.

—— 1976, Preliminary geologic map of the Hermosa Peak quadrangle, Dolores, San Juan, LaPlata, and Montezuma Counties, Colorado: U. S. Geol. Survey Open-File Rept. 76–314.

Pratt, W. P., McKnight, E. T., and De Hon, R. A., 1969, Geologic map of the Rico quadrangle, Dolores and Montezuma Counties, Colorado: U. S. Geol. Survey Geol. Quad. Map GQ-797.

Ransome, F. L., 1901, The ore deposits of the Rico Mountains, Colorado: U. S. Geol. Survey, 22d Ann. Rept., pt. 2, p. 229–398.

Rickard, T. A., 1897, The Enterprise mine, Rico, Colorado: Am. Inst. Mining Engineers Trans., v. 26, p. 906–980.

Wallace, S. R., MacKenzie, W. B., Blair, R. G., and Muncaster, N. K., 1978, Geology of the Urad and Henderson molybdenite deposits, Clear Creek County, Colorado, with a section on a comparison of these deposits with those at Climax, Colorado: Econ. Geol., v. 73, p. 325–368.

Wallace, S. R., Muncaster, N. K., Jonson, D. C., MacKenzie, W. B., Bookstrom, A. A., and Surface, V. E., 1968, Multiple intrusion and mineralization at Climax, Colorado, *in* Ridge, J. D., ed., Ore deposits of the United States, 1933–1967 (Graton-Sales vol.): New York, Am. Inst. Mining Metall. Petroleum Engineers, p. 605–640.

rock fragments, commonly of volcanic origin, and chert exceed quartz grains, and plagioclases exceed alkali feldspars. In the southern part of the basin, the reverse is true: quartz exceeds rock fragments, which here are commonly of intrusive origin, and alkali feldspars exceed plagioclases. The sandstones in the central part of the basin are more like those in the northern than southern part, but are distinguished by the presence of a green hornblende, which does not occur elsewhere. No stratigraphic changes in mineralogy are apparent.

These three geographic mineralogic groupings suggest that there were at least three different source areas for the detritus in the Lance sandstones in the Powder River Basin. The general flow directions recorded in the channel sandstones indicate the general directions of those sources: a volcanic source to the northwest for the northern part of the basin, and exposed intrusive sources to the west and southwest, respectively, for the central and southern parts of the basin.

ANOMALOUS COPPER IN THE LOWER YELLOWJACKET FORMATION (MIDDLE PROTEROZOIC), EAST-CENTRAL IDAHO

№ 133032

CONNOR, Jon J., U.S. Geological Survey, Box 25046, Denver Federal Center, MS 905, Denver, Colorado 80225

The lower part of the Yellowjacket Formation in east-central Idaho consists of some 3300(?) m of interbedded gray to dark-greenish-gray, fine-grained quartzite, siltite, argillite, and scapolite-bearing marble. The sequence is dominated by thin-bedded to laminated argillitic siltite that displays locally abundant normal grading and ripple cross-laminae. The strata were apparently deposited below wave base. Polygonal mud cracks are present but quite rare, and the expected associated shallow water indicators (e.g., rip-up clasts) are absent. The lower part of the Yellowjacket may be, at least in part, a lateral facies of the overlying middle part, near the top of which lies the world-class Blackbird copper-cobalt-gold deposit.

Anomalous copper is widespread in dark, probably pyritic, argillitic siltite of the lower Yellowjacket. The copper occurrences are small and, apparently stratabound. They are reminiscent of the "green bed-type" of copper occurrences in Belt Supergroup rocks of northwest Montana, but differ from them in lacking both intercalated red (oxidized) strata and an associated silver anomaly. The lower Yellowjacket copper occurrences may be syngenetic and could represent the initial stages of sea-floor venting, which ultimately resulted in the formation of the nearby Blackbird deposit.

VOLCANOLOGY OF THE WEST-CENTRAL MORMON MOUNTAIN VOLCANIC FIELD

№ 133779

CONWAY, F. Michael, Geology Dept., Northern Arizona University, Flagstaff, AZ 86011

The Tertiary Mormon Mountain Volcanic Field (MMVF), of central Arizona, contains a diverse array of volcanic landforms, lithologies, and eruption types. Stratigraphic relationships in the MMVF generally indicate early basaltic activity followed by emplacement of andesitic flows and domes. Hawaiian to Strombolian volcanic activity resulted in basalt lavas, scoria and lava cones, and small shield volcanoes. Sheet lavas of olivine-clinopyroxene basalt form the floor of the field, and volumetrically dominate the field. These flows were emplaced by effusive eruptions along N and NW trending fissures. The largest scoria cone is Apache Maid Mountain. Its evolution from Strombolian activity to a more effusive style of eruption is evidenced by the presence of numerous late-stage basalt flows. North of Apache Maid Mountain lies a small shield volcano composed of multiple basalt lava flows, with associated agglutinate and scoria, erupted from a NW-trending summit. Style of eruption ranges from Hawaiian to Strombolian. The largest andesitic structures of the west-central MMVF are products of Peléan eruptions. Round Mountain is a compound endogenous dome composed of hornblende andesitic lavas and breccias. Table Mountain is lithologically similar to Round Mountain but is composed of short, thick lava flows.

The diversity and timing of volcanic landforms in the west-central MMVF indicates evolution from quiescent volcanism (Hawaiian and Strombolian activity) to more explosive volcanism characterized by Peléan activity. This style of volcanism is similar to volcanism of the nearby San Francisco Volcanic Field and other adjacent fields along the southern Colorado Plateau.

GASTROPOD-BEARING PALEOSOLS OF THE EOCENE WILLWOOD FM. (CLARK'S FORK BASIN, NORTHWESTERN WYOMING): OCCURRENCE, PETROLOGY, AND GASTROPOD TAPHONOMY

№ 130394

CREIGHTON, Ann. Campus Box 315, Univ. of Colorado, Boulder, CO 80309

Limestones of Clarkforkian age in the Clark's Fork Basin, northwestern Wyoming, have produced a significant collection of fossil terrestrial snails. Emphasizing taphonomy's constructive contributions to sedimentological studies, the gastropod localities are placed within the context of their stratigraphic position and their relation to paleosols in a fluvial sequence. Well-preserved gastropods invariably occur within highly calcareous mud lenses. These lenses are associated with drab-colored crevasse splay and levee depositional units exhibiting little or no pedogenic modification, and formed under presumably high relative aggradation rates. Gastropods were not observed in sands, nor in association with any but the most immature paleosols (stage 1). Petrographic thin-section analysis of both the limestone lenses and their lateral units provide information concerning timing of the carbonate emplacement, and the gastropod preservation. By accepting taxonomic uniformitarianism, family-level affinities of the fossil gastropods to modern land snails allows for paleoenvironmental reconstructions. Preservation of the gastropods appears linked to factors such as proportions of pedogenesis vs. sediment accumulation rate, calcium carbonate availability, and features of land snail micro-habitats and behaviorial ecology.

SOURCES AND RATES OF PLANT ACCUMULATION IN DEPOSITS FROM RECENT ERUPTIONS OF MOUNT ST. HELENS

№ 135457

CROSS, Aureal T. and TAGGART, Ralph E., Department of Geological Sciences, Michigan State University, East Lansing, MI 48824-1115

Recent eruptions of Mt. St. Helens provide some modern analogues for interpretation of different types of fossil deposits in Tertiary volcanic terrains. The earthquake and explosive eruption of May 18, 1980, and ensuing eruptions emplaced plant debris by five basic types of depositional mechanisms: 1) Debris avalanche, triggered by an earthquake cascaded down the cone and moved as much as 23 km down valley in about 10 minutes; 2) Mudflows (lahars) and debris flows, mobilized from debris avalanche material and volcanic ash, extended down several valleys including 75 km to the Columbia River over a period of 15.5 hrs.; 3) Direct and channeled blasts from phreatic explosions destroyed most of the vegetation over an area of 500 km^2, removing, transporting, and depositing material in a period of a few seconds; 4) Pyroclastic flows carried lapilli, bombs and all sizes of plant debris aloft depositing this randomly in topographic lows within a few hours; 5) Ash falls buried soil surfaces, forest litter and low plants in proximal regions and also carried scorched needles, twigs and cones over 75 km in a 110^0 arc in less than an hour after the phreatic explosion.

Some of the deposits are in multiple layers with varying amounts of plant debris in different layers, particularly blast and pyroclastic flow deposits; some stumps are buried in situ and others are excavated. Some of the wood is charred and some is deeply eroded on one side facing pyroclastic and blast flow sources. Plant debris formed ebb flow mats in mudflows 60 km from the crater. Decay and degradation of the organic detritus has already begun to remove much of the finely shredded wood and leaf material but it is too early to evaluate the extent to which plant material will be preserved in the various types of deposits.

EFFECTS OF VOLCANIC ASH LAYERS ON MACERAL AND INORGANIC COMPOSITION OF THE C COAL BED, FERRON SANDSTONE MEMBER (CRETACEOUS), MANCOS SHALE, UTAH

№ 130905

CROWLEY, Sharon S., STANTON, Ronald W., SIMON, Frederick O., U.S. Geological Survey, 956 National Center, Reston, VA, 22092

Volcanic ash layers (tonsteins) influenced both the maceral and inorganic composition of coal samples of the C coal bed, Ferron Sandstone Member (Cretaceous) of the Mancos Shale, Utah. Coal samples underlying the tonstein contain more inertinites (40 volume percent--dominantly semifusinite) than coal samples directly above the tonstein (20 volume percent). Vitrinites (dominantly desmocollinite) are generally more abundant in coal samples overlying the tonstein than in samples underlying the tonstein. Semifusinite, an indicator of oxidation and desiccation, suggests that prior to the ash fall, peat developed in a relatively well drained swamp environment. Following the ash fall, the increase in vitrinites (particularly desmocollinite) indicates a change to an environment with restricted drainage, perhaps caused by the volcanic ash, which formed a semi--impermeable layer and ponded surface water.

Previous workers report that tonsteins in the C coal consist primarily of kaolinite and smectite formed by leaching and remineralization of the original volcanic ash layer. Our preliminary analyses of elemental distributions in rock partings and coal (on an ash basis) generally support this hypothesis. Be, Zr, Mg, and Ba contents increase in coal samples nearest the tonstein. In contrast, silica, which also should have been intensively leached from the ash, does not increase nearest the tonstein, which suggests that it was more mobile than the other elements. The distribution of Na, Li, K, Ca, and Sr was not affected by the tonstein.

THE PLIOCENE PALEOTHERMAL ANOMALY AT RICO, COLORADO IS RELATED TO A MAJOR MOLYBDENUM DEPOSIT

№ 129042

CUNNINGHAM, C. G., U.S. Geological Survey, Reston, VA 22092; NAESER, C. W., U.S. Geological Survey, Box 25046, MS 963, Denver Federal Ctr., Denver, CO 80225; CAMERON, D. E., P. O. Box 250, Rico, CO 81332; BARRETT, L. F., 3006 East Hinsdale Ave., Littleton, CO 80122; WILSON, J. C., Applied Resources Ltd., P. O. Box 10894, Denver, CO 80210; and LARSON, P. B., Dept. of Geology, Washington State Univ., Pullman, WA 99164

A major paleothermal anomaly is present around the Silver Creek molybdenum deposit at Rico, Colorado. Fission-track ages in apatite and zircon from Laramide-age hornblende-latite sills have been partially reset as far away as 6 km. The reset ages become systematically younger toward the center of the hydrothermal system and approximate a "bullseye" over the molybdenum deposit and its associated alaskite dikes. The molybdenum deposit is 3-5 Ma and the hornblende-latite sills in the Rico district closest to the site of the deposit give Pliocene ages from apatite and zircon that were totally reset. The paleothermal

anomaly extends more than twice as far as epithermal silver, lead, and zinc vein and replacement deposits that are peripheral to the molybdenum deposit.

The molybdenum deposit, which was recently discovered by the Anaconda Minerals Co., contains approximately 44 million tons of 0.31% Mo. Projections of the 0.2% Mo outline indicate that the deposit may contain more than 200 million tons. The ore body is in Precambrian quartzite and greenstone and was localized along the axis of the Rico dome by major faults. The top of the ore body is 1,200 m below Silver Creek near the east end of the Rico district. Fluid inclusions in the veins have homogenization temperatures of 200°-300°C and salinities less than 5 wt % NaCl, whereas those in the molybdenum deposit give 350°-420°C with variable salinities. Stable isotopes indicate that meteoric water is dominant in the epithermal vein systems, but that magmatic water is dominant in the molybdenum deposit.

EPIGENETIC SILVER-LEAD-ZINC MINERALIZATION IN THE CARRIETOWN MINING DISTRICT, BLAINE AND CAMAS COUNTIES, IDAHO

№ 129826

DARLING, Robert S., MOYE, Falma J., BLOUNT, Charles W., and LINK, Paul K., Dept. of Geology, Idaho State University, Pocatello, Idaho 83209

The Carrietown silver-lead-zinc district is located in the central Smoky Mountains of south-central Idaho, on the southwestern margin of the Central Idaho Black Shale Mineral Belt of Hall (1985). In the district, Permian Dollarhide Formation structurally overlies Paleozoic(?) Carrietown sequence in thrust fault contact. Both tectonostratigraphic units are intruded by Cretaceous granodiorites of the Idaho Batholith and by Eocene hypabyssal dacite porphyry dikes and small stocks associated with the Challis magmatic episode.

The ore bodies occur as northeasterly trending vein-type fracture fillings and replacements in both the Dollarhide and the Carrietown. Most deposits, however, are located in proximity to the thrust fault or contacts with Cretaceous granodiorites. The deposits are composed principally of argentiferous galena and sphalerite, accompanied by pyrite, arsenopyrite, chalcopyrite and tetrahedrite. Ores hosted by the Dollarhide have a quartz-calcite gangue in contrast to those hosted by the Carrietown which have a quartz-siderite gangue. These minerals generally occur in brecciated fault zones, and open-space filling textures are common. Thus, the deposits are interpreted as epigenetic. However, sulfides contained within them were probably remobilized from fine-grained stratiform syngenetic sulfides found in both the Dollarhide and the Carrietown.

Field relations and textural evidence suggest only one period of epigenetic mineralization, probably related to either Cretaceous or Eocene plutonism. The spatial relationship of some deposits to locally sericitized granodiorites suggests a Cretaceous age. This age is further supported over an Eocene age because unmineralized/unaltered dacite porphyry dikes cut mineralized structures. However, the Idaho Batholith is believed to have been emplaced at mid-crustal levels (15-20 km), depths not consistent with an apparently shallow ore-forming environment as suggested by the open-space filling textures. Therefore, these textures suggest that either: (1) the deposits formed under Eocene hypabyssal conditions, or (2) if Cretaceous, the depth of emplacement for that portion of the Idaho Batholith is considerably less than currently proposed.

HORIZONTAL STRESS ORIENTATIONS FROM WELL-BORE BREAKOUTS IN THE SOUTH-CENTRAL UNITED STATES

№ 132650

DART, Richard L., U.S. Geological Survey, Box 25046, Denver Federal Center, MS 966, Denver, CO 80225

Dipmeter and fracture-identification well logs from 165 oil and gas wells in a study area extending from the Texas Panhandle to the Mississippi River (including Oklahoma and Arkansas) yield information on the orientation of horizontal crustal stresses. The stress data are inferred from approximately 1,000 directionally oriented well-bore elongations (breakouts) totalling over 26,000 vertical feet. Within this area, the wells are located in nine structural provinces: the Mississippi Embayment, Arkoma basin, Ouachita fold belt, Anadarko basin, Ardmore-Marietta basins, southern Oklahoma aulacogen, Midland basin, Palo Duro-Dalhart basins, and the Hugoton Embayment.

Wells located in the central part of the study area from Oklahoma to the Mississippi River form a high-quality data set having a consistent north-northwest- to north-trending orientation indicative of an east-northeast regional maximum horizontal compressive stress ($S_H$max) direction. These data agree with a $S_H$max orientation of N. 65° E. based on a hydrofracture study in central Oklahoma. This high-quality data set includes breakout orientations from wells in south-central Oklahoma in the vicinity of the west-northwest-striking Meers fault. The east-northeast regional $S_H$max is compatible with evidence of Holocene left-lateral oblique slip on the Meers fault. Possible deviation from this regional stress trend is seen in the orthogonal northwest and northeast distribution of breakouts in wells in the southwestern part of the study area. This apparent local deviation could be related to a complex tectonic and structural history. However, it is possible that hydraulically induced fracturing during drilling may be seen as breakouts on fracture-identification well logs. If this is the case, this orthogonal data might be compatible with the regional $S_H$max; that is, northwest-oriented breakouts are normal to the regional $S_H$max while northeast-trending breakouts may in fact be hydraulic fractures oriented subparallel to it. Elsewhere within the study area, variations in breakout orientations preclude a determination of current stress directions.

CONODONT BIOSTRATIGRAPHY OF THE LAKE POINT LIMESTONE AND RECOGNITION OF THE MISSISSIPPIAN/PENNSYLVANIAN BOUNDARY AND A POTENTIAL MORROWAN STRATOTYPE.

№ 126115

DAVIS, Larry E., and WEBSTER, G.D., Dept. of Geology, Washington State University, Pullman, WA 99164

The Lake Point limestone, located in the northern Oquirrh Mountains of northern Utah, is a nearly continuous sequence of bioclastic limestones and calcareous sandstones deposited on a carbonate shelf within the rapidly subsiding Oquirrh Basin. These limestones have yielded relatively high diversities of platform conodont elements. The upper part of the Chesterian *Adetognathus unicornis* and the *Rhachistognathus muricatus* biozones are present. Other Chesterian conodonts include *Cavusgnathus naviculus, C. unicornis, C. regularis, Gnathodus girtyi simplex, G. bilineatus,* and *Spathognathodus spiculus.*

The Mississippian/Pennsylvanian boundary, recognized at the lowest occurrence of *Rhachistognathus primus*, is 173.1 m above the base of the section. Important Morrowan conodonts present include *Adetognathus gigantus, A. lautus, A. spathus, Declinognathodus noduliferus, D. japonicus, D. inaequalis, Idiognathoides corrugatus, Id. sinuatus, Id. sulcatus parvus, Id. sulcatus sulcatus, Neognathodus symmetricus, R. minutus havlenai, R. minutus minutus, R. prolixus, and R. webster*i, and enable the recognition of most Morrowan conodont biozones.

The Morrowan/Atokan boundary is interpreted to coincide with the first appearance of *Diplognathodus coloradoensis.* The presence of *D. coloradoensis, Idiognathoides marginodosus,* and *Neognathodus atokanensis* clearly place the upper 78 m of the Lake Point Limestone in the Lower Atokan.

In addition to conodonts, these limestones also yielded excellent brachiopod faunas and to a lesser extent foraminifera, corals, and bryozoans. Recognition of these boundaries within the unit, makes the Lake Point Limestone a candidate for Mid-Carboniferous and a Morrowan stratotype in the eastern Great Basin.

DIKE EMPLACEMENT AND SILICIFICATION OF PALEOZOIC SEDIMENTARY ROCKS IN THE NORTHERN LOST RIVER RANGE, IDAHO

№ 124375

DAVIS, Linda C., Department of Geology, Idaho State University, Pocatello, ID 83209

Lower to mid-Paleozoic limestone, dolomite and quartzite near Mahogany Hill, in the northern Lost River Range, east-central Idaho, have undergone silicification and intrusion by dikes. The study area is located on the eastern flank of the range, approximately 6 miles north of Doublespring Pass, on the west side of the Pahsimeroi Valley. This area is on the Lost River Plate, one of several Mesozoic allochthons in east-central Idaho. Basaltic and andesitic flows, pyroclastics, and dikes of the Eocene Challis Volcanics unconformably overlie the Paleozoic rocks in the area. Basin and Range extensional faulting is still active as evidenced by eastward tilt of the range associated with the magnitude 7.3 Borah Peak earthquake along the Lost River Fault in October, 1983.

Previously unmapped, highly altered, purplish-red porphyritic dikes, possibly associated with the Challis Volcanics, intrude folded and faulted Paleozoic strata. The dikes do not crop out well and are usually defined by concentrations of float in swales. Oxidized zones in the country rock are commonly associated with the dikes and help delineate their trend where no outcrop is found. Most dikes appear to be emplaced along steeply dipping, northeast-trending joint systems in the country rock.

Nonlinear zones of silicification (jasperoid(?)), partially silicified dolomite and limestone, and silicified breccia are spatially associated with the dikes. These zones may be related primarily to faults and secondarily to joints, which acted as conduits for silica-bearing solutions.

THE PETROLOGY AND GEOCHEMISTRY OF THE INTRUSIVE ROCKS AND ASSOCIATED IRON-RICH POLYMETALLIC SKARN AT REILLY PEAK, NEW MEXICO

№ 135119

DAVIS, Linda L., 8960 Carr St., Westminster, CO 80020

Igneous rocks at Reilly Peak, 8 km north of Winston, include intrusive high-silica rhyolite, andesitic lithic tuff, andesite dikes, a basaltic andesite plug and porphyritic rhyolite dikes.

The main part of Reilly Peak is the intrusive high-silica rhyolite (36.0 ± 1.4 m.y.) with trachytic to spherulitic textures. It is highly fractured with mineralogy that reflects high-temperature deuteric alteration and later hydrothermal alteration. Two generations of altered biotites can be distinguished physically and chemically. The compositions of the two generations vary throughout the stock. Interlayer CaO and H_2O have been added to, and K_2O has been depleted from the biotites. The high-silica rhyolite is compositionally similar to rhyolites from bimodal assemblages and to biotite rhyolites of the eastern orogenic belt of the western U.S.A.. The porphyritic rhyolites (22.6 ± 0.8 m.y.) are similar in composition to topaz-bearing rhyolites, however, differences in trace-element abundances and an absence of topaz distinguish the porphyritic rhyolites from topaz-bearing rhyolites. Low-potassium andesite dikes (41.0 ± 7.4 m.y.) in the northern part of the area are much older than the andesites in the southern part.

Emplacement of igneous rocks, with accompanying metamorphism and fracturing, and pre-existing faults provided an environment favorable for the formation of the Fe-F-Sn-W-Be-S-B-Bi-Cu-Zn-Pb skarn deposits. The source of skarn-forming fluids is probably multiple granitic or monzonitic plutons at depth which may be comagmatic with the high-silica rhyolite.

ABSTRACTS with PROGRAMS 1987

40th Annual Meeting

ROCKY MOUNTAIN SECTION

The Geological Society of America

with the
Paleontological Society of America
Rocky Mountain Section

May 2-4, 1987
University of Colorado
Boulder, Colorado

Volume 19, Number 5, March 1987
ISSN 0016-7592

Skip -
Best wishes - are we getting together in Rico this summer?

Economic Geology
Vol. 82, 1987, pp. 2141–2157

Stable Isotope and Fluid Inclusion Investigations of Epithermal Vein and Porphyry Molybdenum Mineralization in the Rico Mining District, Colorado

Peter

PETER B. LARSON

Department of Geology, Washington State University, Pullman, Washington 99164-2812

Abstract

The Rico mining district, western San Juan Mountains, Colorado, contains epithermal vein deposits, carbonate replacement deposits, and a large zone of porphyry-style molybdenum mineralization. Historically, the vein and replacement deposits have produced significant amounts of silver, lead, and zinc, with minor gold and copper. All the mineralization formed nearly contemporaneously about 5 m.y. ago. The veins and replacement deposits occur in Paleozoic and Mesozoic sedimentary rocks that have been uplifted into the Rico dome, which is cored by a horst of Precambrian greenstone and quartzite. The porphyry molybdenum mineralization (40 million tons of 0.31% Mo) is 1,500 m beneath the surface in the east end of the district and consists of stockwork veining in Precambrian quartzite and greenstone and in Pennsylvanian sedimentary rocks. The epithermal veins occur above and peripheral to the porphyry mineralization. Widespread high silica, alaskite porphyry dikes were also emplaced at the same time as the porphyry mineralization and are probably related to the source intrusion for the molybdenum mineralization and the heat source for the hydrothermal system that produced the epithermal and replacement deposits. Fluid inclusions in quartz from the veins homogenize at temperatures in the range 200° to 300°C and yield salinities less than 5 equiv wt percent NaCl. The δD values of quartz inclusion fluids (−112 to −121‰) and calculated $\delta^{18}O$ values of fluids in equilibrium with the quartz (−3 to −17‰) show that the epithermal vein fluids were ^{18}O-shifted meteoric waters. Vein samples with large ^{18}O shifts also exhibit very saline fluid inclusions, indicating that the fluids which experienced the greatest degree of water-rock interaction contain the highest concentration of dissolved components. The porphyry fluid (δD = −90 to −104‰, $\delta^{18}O$ = +2‰) was derived from mixed magmatic and meteoric sources. Primary inclusions in the porphyry veinlets homogenize to both liquid and vapor in the temperature range 350° to 420°C, suggesting that boiling occurred during their formation. Trains of secondary inclusions are abundant in the veinlets and show that a later lower temperature fluid encroached upon the porphyry system. No evidence for mixing of magmatic and meteoric fluids was found in any of the epithermal veins. The porphyry mineralization formed early in the history of the Rico hydrothermal system. Epithermal vein formation occurred later than the porphyry mineralization, and the meteoric-hydrothermal fluid collapsed into the porphyry core of the system during the retrograde stages of the hydrothermal system.

Introduction

OXYGEN and hydrogen isotope analyses of epithermal vein materials typically show that meteoric water is the prevalent hydrothermal fluid reservoir for epithermal vein formation (O'Neil et al., 1973; Taylor, 1973; Casadevall and Ohmoto, 1977; Bethke and Rye, 1979; Robinson and Christie, 1980; Matsuhisa et al., 1985; Brooks et al., 1986; Larson and Taylor, 1987). However, Rye and Sawkins (1974) have shown that magmatic fluids were the dominant component for vein formation at Casapalca, Peru. Minor magmatic components have also been detected in the Creede district, Colorado (Bethke and Rye, 1979). Stable isotope studies of porphyry-type deposits have shown that a magmatic fluid is commonly involved in this style of mineralization (Sheppard et al., 1971; Hall et al., 1974; Sheppard and Gustafson, 1976; Taylor, 1979; Hannah and Stein, 1986).

The Rico mining district, Colorado, contains a diverse assemblage of hydrothermal mineral deposits that includes epithermal Ag-Zn-Pb veins, limestone replacement deposits, and a large porphyry-style molybdenum deposit. The vein and replacement deposits are peripheral to the deep molybdenum mineralization, and radiometric ages and geologic relationships show that all these deposits formed at approximately the same time. This paper reports the results of an investigation to determine the sources of fluids involved in the vein and porphyry mineralization in the Rico district, and to look for evidence of the interaction among these fluids in the hydrothermal system. Oxygen and hydrogen isotope ratios have been measured for minerals and inclusion fluids from the epithermal vein and porphyry deposits. Fluid inclusion homogenization and freezing point measurements for these same samples have also been completed. These data show that two isotopically distinct fluids, one of meteoric

0361-0128/87/762/2141-17$2.50

affinity and one of magmatic affinity, were present in the hydrothermal system. Only an evolved meteoric fluid was involved in the epithermal vein formation, but fluids of mixed heritage produced the porphyry mineralization.

Geology of the Rico District

The Rico district (Fig. 1) is located in the western San Juan Mountains, southwest Colorado, and lies 20 km west of the edge of the San Juan volcanic field. From 1879 through 1968 the district produced 76,064 metric tons of lead, 75,309 tons of zinc, 5,114 tons of copper, 14,513,288 oz of silver, and 83,045 oz of gold (McKnight, 1974; Cameron et al., 1987). The geology and precious and base metal mineral deposits of the district have been described by Cross and Spencer (1900), Ransome (1901), Cross and Ransome (1905), Pratt et al. (1969), and McKnight (1974). Excellent geologic maps of the district are provided by Pratt et al. (1969) and McKnight (1974). Fission track and radiometric ages of intrusive rocks and alteration minerals in the Rico district have been reported by Naeser et al. (1980). The Silver Creek molybdenum deposit in the eastern part of the district was discovered and explored by drilling by the Anaconda Minerals Company in the late 1970s and early 1980s: the geology and exploration history of the molybdenum deposit are described by Cameron et al. (1987).

Geology of the Rico dome

Mineralization in the Rico district occurs within the Rico dome (Fig. 1). The 12 by 12 km dome is cored by a horst of Precambrian quartzite and greenstone and is flanked by a thick section of Paleozoic and Mesozoic sedimentary rocks. Structural contours drawn on the Pennsylvanian-Permian contact show that a minimum of 1,000 m of uplift has occurred. East-west–, northwest-southeast–, and northeast-southwest–striking faults predominate, and two major zones of faulting intersect in the eastern part of the dome (Fig. 1).

Detailed descriptions of the stratigraphic section are provided by Cross and Spencer (1900) and McKnight (1974). The lowermost Paleozoic unit, the Mississipian Leadville Limestone, lies unconformably on quartzites of the Precambrian Uncompahgre Formation. The Leadville Limestone is locally 75 m thick and the top of the unit exhibits widespread karst and related erosional features. A sequence of clastic and calcareous sedimentary rocks up to 1,000 m thick, the Pennsylvanian Hermosa Group, overlies the Leadville Limestone. In Rico the Hermosa Group is locally subdivided into three members. The lower member displays a variable thickness and a diverse assemblage of marine

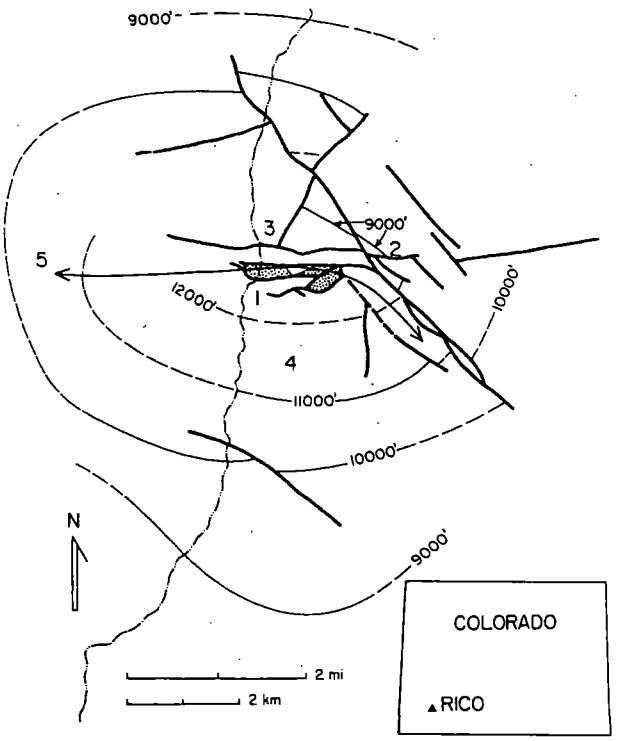

FIG. 1. Structural map of the Rico district. The Dolores River flows to the south and has deeply incised the central portion of the dome. Structural contours, drawn on the Pennsylvanian-Permian contact, show that about 3,000 ft (1,000 m) of uplift has occurred. Major faults (heavy lines) and the central horst of Precambrian rocks (stippled pattern) are also shown. Mineralized areas discussed in the text are: (1) lower Silver Creek, (2) Silver Creek molybdenum deposit and the Argentine mine (upper Silver Creek), (3) CHC Hill-NBH, (4) Newman Hill, and (5) Calico Peak.

clastic lithologies that varies from siltstones to coarse arkosic sandstones. The middle member contains about 30 percent thin limestone units interbedded with arkosic sandstones. The upper member consists of arkose, shale, sandstone, and conglomerate, with minor interbedded limestone. Red beds of the Pennsylvanian Rico Formation and the Permian Cutler Formation overlie the Hermosa Group on the edges of the Rico dome, but they have been removed by erosion over the central part of the uplift.

Igneous rocks emplaced during two episodes of Cretaceous-Tertiary magmatism are present in the Rico district (McKnight, 1974; Naeser et al., 1980). An augite monzonite stock and numerous hornblende latite sills and dikes are Cretaceous-Paleocene (Laramide) in age and intrude the Paleozoic and Mesozoic sedimentary rocks. The augite monzonite forms a 2.5-km-diam stock in the west-central part of the dome. Naeser et al. (1980) report a 78-m.y. sphene fission-track age for the augite

monzonite. The hornblende latite sills and dikes are widespread throughout the district. Zircon fission track ages of 59.9 to 64.9 m.y. for the latite (Naeser et al., 1980) indicate that the latite is younger than the monzonite, although definitive crosscutting relationships have not been found in the field. Several samples of the latite and monzonite studied by Naeser et al. (1980) yielded younger fission-track ages than those noted above: these were interpreted by these authors to have been thermally reset.

The second episode of magmatism resulted in the emplacement of a series of Pliocene dikes and small stocks that includes lamprophyres, basalt, and alaskite porphyry. Two zircon ages of 3.4 and 3.9 m.y. for the alaskite porphyry were reported by Naeser et al. (1980). Cameron et al. (1987) dated an alaskite dike collected from drill core. This sample yielded a K-Ar age of 5.2 m.y. The alaskite porphyry is believed to be the source for the porphyry molybdenum mineralization (Naeser et al., 1980; Cameron et al., 1987). A small stock and several dikes of a distinctive porphyrytic rock with large orthoclase and resorbed quartz phenocrysts, the Calico Peak Porphyry, are exposed near the western edge of the dome. Naeser et al. (1980) measured a biotite K-Ar age of 4.5 m.y. for one of these intrusions.

Mineralization in the Rico district

Hydrothermal mineralization at Rico occurs in a diverse assemblage of deposits. All these deposits appear to be contemporaneous with, or slightly younger than, emplacement of the alaskite porphyry dikes. Hydrothermal alteration minerals have been radiometrically dated in one location, along a meter-wide quartz vein that directly overlies the deeper porphyry molybdenum deposit by about 1,500 m. Two samples of sericite collected along the vein walls yielded K-Ar ages of 5.45 and 5.39 m.y. (Naeser et al., 1980). An outcrop of the alaskite porphyry, 500 m northeast of the dated selvage, has been explored by a short adit. Here, the porphyry is pervasively altered and cut by centimeter-wide veins of quartz, pyrite, sphalerite, and galena. The alaskite porphyry is similarly altered in all other exposures throughout the mineralized portion of the district; locally the porphyry is cut by thin stringers of quartz and pyrite.

Mineralization styles in the Rico district include epithermal vein, carbonate replacement, and porphyry molybdenum deposits. Mineralization has also occurred in porous evaporite horizons in the lower Hermosa Group sedimentary rocks, where these horizons are intersected by the epithermal veins. Early in the history of the district miners named these horizons "contacts." This uncharacteristic usage is maintained in this paper. One area of solfataric alteration with enargite and pyrite pods is present at Calico Peak on the west end of the dome (Larson and Taylor, 1987). Nearly all of the deposits are now inaccessible, and the following descriptions are drawn from Ransome (1901), McKnight (1974), and Cameron et al. (1987) and from observations of core and old dump material. Areas of mineralization referred to in the text are located in Figure 1.

Veins and contacts: Quartz veins fill fractures and faults throughout the district. The quartz is generally vuggy and exhibits inward-projecting terminations from the vein walls. Pyrite is widespread in the veins and sphalerite, galena, and chalcopyrite are also common. Rhodonite and rhodochrosite are common vein minerals on Newman Hill, where they occur banded with the quartz and sulfide minerals. The manganese minerals are much less common in other areas, such as CHC Hill. Silver sulfide minerals also occur in the Newman Hill veins, which produced a large amount of silver early in the history of the district. Throughout the district the veins are best developed in the lower and middle members of the Hermosa Group sedimentary rocks. Veins are also well developed in faults that bound and crosscut the Precambrian horst in the center of the dome.

Several contacts were discovered by the early miners, but only the Enterprise contact on Newman Hill in the lower Hermosa Group proved to be highly productive. Ransome (1901) provides an excellent description of this contact and he attributes to it a third of the district's production through 1901. The Newman Hill veins fill faults and fractures (Fig. 2) in which mineralization terminates upward at the contact. The Newman Hill veins were only productive for about 30 m below the contact and only the northeast-trending veins were economically mineralized. Although the structures that the veins filled persist above the contact, no veins were developed in these hanging-wall fractures. Long tabular orebodies consisting of the same minerals that are found in the veins formed in the contact where it is intersected by a vein. Typically the contact is 2 m thick. Massive gypsum occurs between the tabular orebodies, and many natural caves were discovered by the miners in the gypsum and in the spaces between the gypsum and the ore. The surface of the gypsum exhibits extensive solution cavities, which are well illustrated by a photograph in Ransome's report (plate XXXII, Ransome, 1901). The overlying bedded siltstone has slumped extensively into the solution cavities. McKnight (1974) notes that bedded evaporite deposits are common in the lower Hermosa Group southwest of

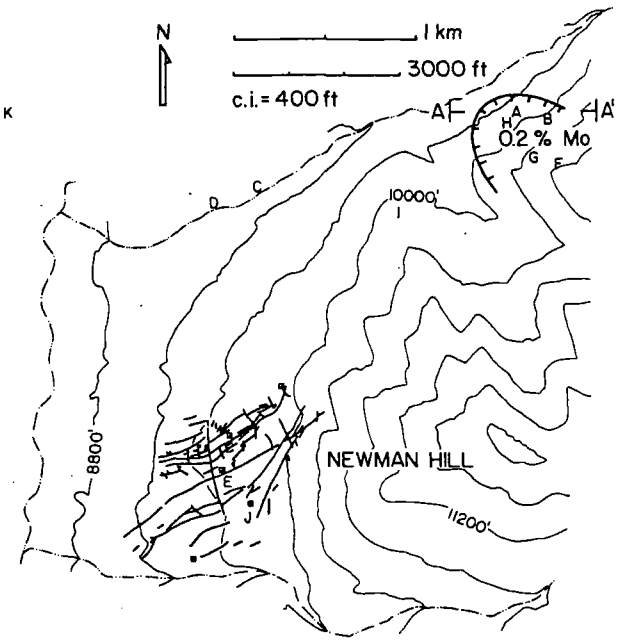

FIG. 2. Topographic map of the southeastern area of the Rico district showing the location of the Newman Hill veins (from Ransome, 1901), and the Silver Creek molybdenum deposit 0.2 percent Mo cutoff (from Cameron et al., 1987) projected to the surface. Also shown are sample locations as designated by the corresponding letters (A–K) in Table 3. See Figures 3 and 4 for cross section A-A'.

the Rico dome, and he attributes the gypsum in the Enterprise contact to a sedimentary origin.

Sequential deposition of vein minerals from which paragenetic relations can be discerned are found only in the Newman Hill veins. Here, three distinct paragenetic zones have been defined. Zone I, generally less than 1 cm wide, consists of a band of terminated quartz crystals along the vein walls. Minor euhedral pyrite usually accompanies the quartz. Zone II is younger than zone I and typically exhibits alternating bands of quartz and rhodochrosite with local pods of sulfide minerals. Zone II quartz is euhedral and can occur as rosettes or in a cockscomb texture. This zone varies from 2 to greater than 10 cm wide, and some samples contain individual quartz crystals up to 5 cm in length. The most abundant sulfide minerals are galena, sphalerite, and pyrite; chalcopyrite is less common but ubiquitous. Argentite is present in minor amounts, generally in association with chalcopyrite. The sphalerite is rarely zoned but commonly contains small grains of chalcopyrite (chalcopyrite "disease") that are distributed along growth planes. Tetrahedrite is also found as small stringers in the sphalerite. In addition to these minerals, Bastin (1922) found tennantite, proustite, polybasite, and pearceite in the veins, and McKnight (1974) reports the occurrence of stephanite, native gold, and native silver. Minor rhodonite accompanies the rhodochrosite. Zone II varies from 2 to greater than 10 cm wide. Zone III is the youngest zone and fills the center of the veins. It consists of massive quartz with inward-projecting terminations. Minor rhodonite, sphalerite, galena, and pyrite are also present.

Veins in lower Silver Creek are less than 0.5 m wide and are not zoned. Quartz is the most abundant mineral in these veins and often is the only mineral present. In some places bladed specular hematite, partially replaced by magnetite, occurs together with minor pyrite, galena, and sphalerite. In upper Silver Creek, veins along the Blackhawk fault in the Argentine mine vary from 0.5 to 2 m wide and consist of massive quartz and calcite with only minor pyrite.

Limestone replacement deposits: Replacement deposits in limestone beds in the Rico district themselves exhibit a great diversity. Two distinct types have been found:

1. Massive pyrite with minor galena, chlorite, and clay replaces the middle Hermosa Group limestones along quartz veins in the Argentine and CHC Hill areas (Fig. 1). Pyrite in these deposits was mined as a source of sulfuric acid in the 1950s and 1960s. Locally these replacements contain sphalerite and galena, minor chalcopyrite, tetrahedrite, quartz, carbonate minerals, fluorite, and rare alabandite and cosalite. These replacements were important sources of lead, zinc, and silver.

2. Massive replacement of the Leadville Limestone is found in lower Silver Creek. In one example at the Atlantic Cable mine (McKnight, 1974), massive specularite, magnetite, and chlorite replace the dolomitized limestone. Silicification is also locally important. Pods of sphalerite, galena, and chalcopyrite are scattered through the massive gangue minerals. These deposits produced significant amounts of silver early in the history of the district. A similar deposit, the NBH zone, north of the lower Silver Creek area, was discovered by drilling in the 1960s. Drilling encountered overpressured hot brines in the mineralized zone. The NBH deposit contains abundant pyrite and chalcopyrite in addition to iron oxides and other gangue minerals. The lower Silver Creek replacement deposits may also be controlled by porous remnant karst features at the top of the Leadville Limestone.

Porphyry molybdenum deposit: Exploration diamond drilling by the Anaconda Minerals Company from 1978 through early 1983 resulted in discovery of the Silver Creek molybdenum deposit (Cameron et al., 1987) in the east end of the Rico district. The deposit lies about 1,500 m beneath the surface in

the upper Silver Creek area. Reserves indicated by drilling are 40 million tons of 0.31 percent Mo. The mineralization is not closed on its southeastern side, and total potential reserves may be 200 million tons (Cameron et al., 1987). The surface projection of the 0.2 percent Mo cutoff is shown in Figure 2. An east-west cross section through the deposit (Fig. 3) shows the relatively flat, tabular shape of the mineralized zone. The highest grade mineralization occurs along the contact of the Precambrian Uncompahgre Quartzite with the overlying Hermosa Group and the underlying Precambrian greenstone. In plan view the high-grade zone straddles the Last Chance fault. A source intrusion has not been intersected by drilling. The alaskite porphyry dikes occur only in the eastern half of the district and were infrequently encountered during drilling.

The mineralization occurs as characteristic stockwork quartz-molybdenite veinlets. A detailed discussion of alteration associated with the molybdenum deposit is presented by Cameron et al. (1987). Veinlet-related alteration (Fig. 4) consists of a deep potassic zone in which secondary biotite and locally orthoclase pervasively invades the walls. Local quartz-orthoclase veinlets are also present. Anhydrite commonly accompanies the biotite and occurs with quartz in early veinlets in the upper part of the zone. The potassic alteration grades upward to a typical quartz-sericite-pyrite phyllic zone. This in turn grades upward to a propylitic facies best characterized by the development of hydrothermal chlorite, calcite, epidote, and pyrite in the hornblende latite porphyry throughout the district. Paleozoic carbonate rocks above the Uncompahgre Quartzite have been replaced by garnet and minor diopside. This is in turn overlain by a zone in which massive diopside and massive anhydrite replace carbonate units. Cameron et al. (1987) suggest that the massive anhydrite predates formation of the calc-silicate alteration.

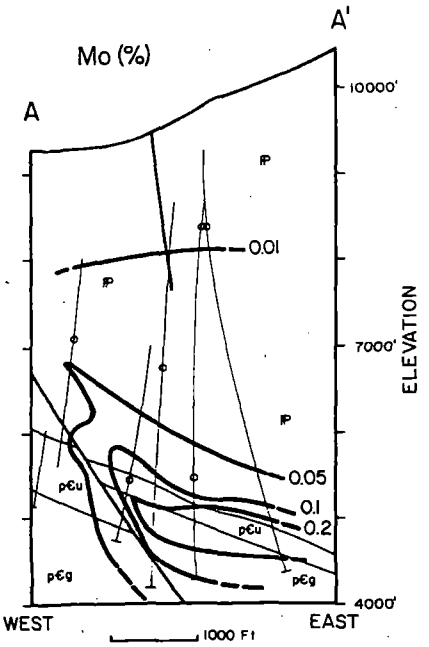

FIG. 3. Cross section A-A' (Fig. 2) showing Mo grades (from Cameron et al., 1987). Drill holes are projected to the plane of the cross section and are shown as thin lines. The piercing point for each hole is shown as a small circle. The geologic units are: pCg, Precambrian greenstone; pCu, Uncompahgre quartzite; P, Paleozoic sedimentary rocks. Faults are shown as medium heavy lines.

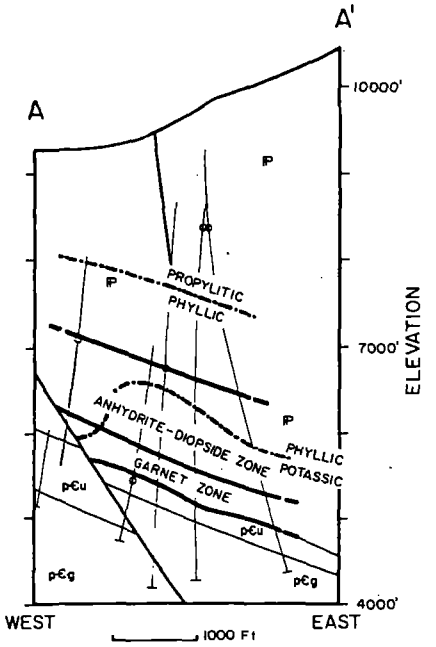

FIG. 4. Cross section A-A' (Fig. 2) showing alteration facies associated with the Silver Creek molybdenum deposit (from Cameron et al., 1987). See Figure 3 for an explanation of symbols and geologic units. Carbonate beds in the lower Paleozoic section are altered to garnet near the high-grade molybdenum zone and to massive anhydrite and diopside peripheral to the garnet zone. Veinlet-related alteration consists of a proximal potassic facies and a distal phyllic facies, which grades upward and outward to a district-wide pervasive propylitization.

Sampling and Analyses

Samples from veins in lower Silver Creek, from Newman Hill, and in upper Silver Creek over the top of the Silver Creek molybdenum deposit were collected and have been analyzed. Core samples of quartz-molybdenite from the molybdenum deposit were also collected and analyzed. Core samples are catalogued by the drill hole number and the depth in feet below the drill collar from which the sample of core was collected. The lower and upper Silver

Creek veins were sampled in place (Fig. 2). Newman Hill is covered with Pleistocene landslide debris (Cross and Spencer, 1900; McKnight, 1974) and the old mine workings are caved and inaccessible. The Newman Hill samples were collected by carefully examining and selecting vein samples from the old mine dumps. Comparison of slabbed dump samples to the line drawings of Newman Hill veins in Ransome (1901) shows that these samples are typical of those veins. It was possible to collect samples of the Newman Hill veins that are complete from wall to wall.

Greater than 99 percent pure quartz was hand picked from crushed samples of the veins. Oxygen isotope analyses were conducted at Caltech using fluorine gas as a reacting agent, essentially according to the technique of Taylor and Epstein (1962). All results are reported in the familiar δ notation in per mil. Precision is better than 0.2 per mil. Raw δ values are corrected to the SMOW scale using the Caltech rose quartz δ value of 8.45; National Bureau of Standards-28 has a $\delta^{18}O$ value of 9.60 per mil on this scale. Hydrogen isotope analyses of inclusion fluids were conducted at the U. S. Geological Survey laboratory at Menlo Park by thermal decrepitation of −160 mesh crushed quartz at 1,300°C. Water released during decrepitation was reacted with zinc to produce hydrogen gas. The δD values are reported in per mil relative to SMOW, with precision better than 1 per mil. Doubly polished chips of vein material were prepared for fluid inclusion heating and freezing measurements using a gas flow heating-freezing stage at Washington State University.

Fluid Inclusion Measurements

Homogenization temperature (T_h) and freezing point depression (T_m) measurements were conducted on fluid inclusions to determine the temperatures of vein and veinlet formation and to place constraints on the compositions of the hydrothermal fluids. Polished quartz chips of samples from Newman Hill, lower Silver Creek, the Argentine mine, and the Silver Creek molybdenum deposit were analyzed. Average T_h values are presented in Table 1, and T_m and T_h for individual inclusions are tabulated in Table 2.

Newman Hill veins

Two vein samples from Newman Hill, RI-011 from the Jumbo shaft and RI-023c from the Vestal shaft, were chosen for detailed study because they exhibit complete cross sections of the three paragenetic zones. Fluid inclusions are common in quartz from each of the three paragenetic sequences in both samples. The inclusions range up to 25 μ in diameter. Primary and secondary inclusions are present in all three zones in both samples. Primary inclusions occur along growth planes parallel to the faces of euhedral quartz crystals. Coarse inclusions that do not lie within linear trains of inclusions are also interpreted to be primary. Secondary inclusions occur in linear trains that commonly

TABLE 1. Average Fluid Inclusion Homogenization Temperatures (T_h) for Vein and Veinlet Quartz from the Rico District

Sample no.	Origin	Average T_h (°C)	Number of measurements	Standard deviation
Quartz-molybdenite veinlets				
SC-5 4168	P/S	315	39	30.2
SC-5 4314	P/S	338	29	42.4
SC-5 4409	P/S	355	30	32.3
SC-7a 4681	P/S	328	19	32.4
SC-7a 4735	P/S	315	28	32.6
SC-7a 5005	P/S	302	19	31.9
Epithermal veins				
RI-003a	S	214	59	22.2
RI-011 I	P	246	12	8.8
	S	289	5	31.3
RI-011II	P	292	18	11.5
RI-011III	P	244	22	29.7
IR-015b	S	238	30	17.2
RI-015c	S	243	22	23.1
RI-017a	S	242	30	18.9
RI-019a	S	252	27	15.9
RI-020	S	291	24	8.8
RI-023c I	P	272	23	29.8
RI-023c II	P	264	21	24.2
RI-023c III	P	232	32	20.6

Inclusion origin is listed as P if most of the measured inclusions for a particular sample were primary and S if they were secondary

TABLE 2. Homogenization Temperatures (T_h) and Melting Point Measurements (T_m) for Individual Fluid Inclusions in Quartz from the Rico District

Sample no.	Origin	T_h (°C)	T_m (°C)	Equivalent weight percent NaCl
Quartz-molybdenum veinlets				
SC-5 4168	P/S	350	−0.4	0.70
SC-5 4314	P/S	360	+8.0	
SC-5 4409	P/S	320	−2.2	3.69
	P/S	305	−1.1	1.90
SC-7a 4681	P/S	320	−4.6	7.29
	P/S	360	+8.7	
	P/S	350	+9.4	
	P/S	350	+9.6	
SC-7a 4735	P/S	355	−4.4	7.01
	P/S	320	−2.1	3.53
	P/S	285	−0.4	0.70
	P/S	320	−0.4	0.70
	P/S	320	+9.6	
SC-7a 5005	P/S	285	−1.0	1.73
	P/S	265	−0.9	1.56
	P/S	295	−0.6	1.05
	P/S	335	+8.2	
	P/S	335	+8.5	
Epithermal veins				
RI-011 I	P	200	−0.7	1.22
	P	210	−0.6	1.05
	S	310	−2.6	4.32
RI-011 II	P	285	−2.5	4.17
	P	275	−3.1	5.09
RI-011 III	P	230	−1.8	3.05
	P	290	−1.4	2.40
	P	280	−1.0	1.73
	P	220	−0.8	1.39
	P	255	−0.7	1.22
	P	275	−0.6	1.05
RI-015c	P	230	−0.4	0.70
	P	265	−0.1	0.18
	S	265	−0.6	1.05
RI-017a	S	NA	−0.6	1.05
	S	NA	−0.5	0.87
RI-019a	S	NA	−0.2	0.35
	S	NA	0.0	0.00
RI-020	S	270	−1.9	3.21
	S	280	−1.7	2.89
	S	275	−0.9	1.56
	S	285	−1.0	1.73
RI-023c I	P	285	−2.6	4.32
	P	265	−2.6	4.32
RI-023c II	P	255	−2.4	4.01
	P	285	−2.3	3.85
RI-023c III	P	210	−0.6	1.05
	P	210	−0.6	1.05
	P	225	−0.5	0.87
	P	210	−0.5	0.87
	P	210	−0.5	0.87

Origin is abbreviated as P for primary and S for secondary; equivalent weight percent NaCl was calculated from the freezing point depressions according to the equation of Potter et al. (1978); NA = not available

crosscut grain boundaries. Fluid inclusion heating-freezing measurements of the Newman Hill samples were restricted almost entirely to primary inclusions because of the clear distinction between primary and secondary inclusions and because primary inclusions are abundant. Daughter minerals were not observed in any of the Newman Hill inclusions.

No pressure correction has been applied to the

Newman Hill homogenization temperatures. Cameron et al. (1987) estimate that a minimum of 1,200 m of rock has been removed by erosion over the top of the Silver Creek molybdenum deposit. The surface of Newman Hill lies at nearly the exact elevation of the present surface above the molybdenum deposit, and the same lithologic unit is exposed in both areas. A similar minimum amount was probably also removed above the Newman Hill veins. At a depth of 1,200 m a 250°C, 2.0 wt percent NaCl solution would lie along the hydrostatic boiling curve at a pressure of about 95 bars (Haas, 1971). A pressure correction for the fluid inclusions under these conditions would be less than 10°C (Potter, 1977). However, no evidence of boiling was found in any of the Newman Hill samples, and the pressure was probably greater than 95 bars. Doubling this pressure would still result in a pressure correction no greater than 10°C (Potter, 1977).

T_h and T_m values in both samples vary among the three zones. Figure 5 shows these variations for sample RI-011, together with a drawing of a slabbed piece of RI-011 that shows the paragenetic relations of the three zones. The average homogenization temperature of primary inclusions increases from 246°C in zone I to 292°C for zone II, and then drops to 244°C in zone III. In sample RI-023c the average homogenization temperature decreases from zone I (272°C) through zone II (264°C) to zone III (232°C). In sample RI-011 the freezing point of primary inclusions in zones I and III lie within the same range (−0.6° to −1.8°C) but are lower in zone II (−2.5° to 3.1°C). Zones II and III freezing point depressions in RI-023c are similar to those in zones II and III from sample RI-022, but the zone I depressions are lower (−2.55°C).

The presence of carbon dioxide in the inclusion fluids can affect the freezing point of the fluid (Collins, 1979; Hedenquist and Henley, 1985). Inclusions from all three zones from each sample yielded expanded bubbles of carbon dioxide when powdered mineral was crushed in oil between glass plates. However, carbon dioxide was not observed in the uncrushed inclusions in the form of double menisci. The lack of a liquid CO_2 phase in the inclusions places an upper limit of CO_2 concentration at about 2.2 molal at 10°C (Hedenquist and Henley, 1985). At CO_2 concentrations between 0.85 and 2.2 molal, formation of a clathrate during freezing will concentrate salts in the residual liquid phase and result in a decrease in the ice melting point. Although no evidence for a CO_2 hydrate was observed in the inclusions, the salinities calculated from the ice melting temperatures should be considered maximum values.

Three secondary inclusions in zone I of RI-011 probably formed during zone II deposition. These inclusions homogenize about 50°C higher than the average zone I homogenization temperature for this sample (Fig. 5). Their homogenization temperatures lie within the upper range of zone II homogenization. The freezing point temperature of one of these inclusions is −2.6°C, which is within the range of the zone II measurements but is two degrees lower than typical zone I temperatures. These three inclusions probably formed in fractures in the zone I quartz during zone II deposition, and in further discussions they will be included in the zone II data.

Comparison of the fluid inclusion data between the two samples shows that deposition did not follow a consistent thermal history in all the Newman

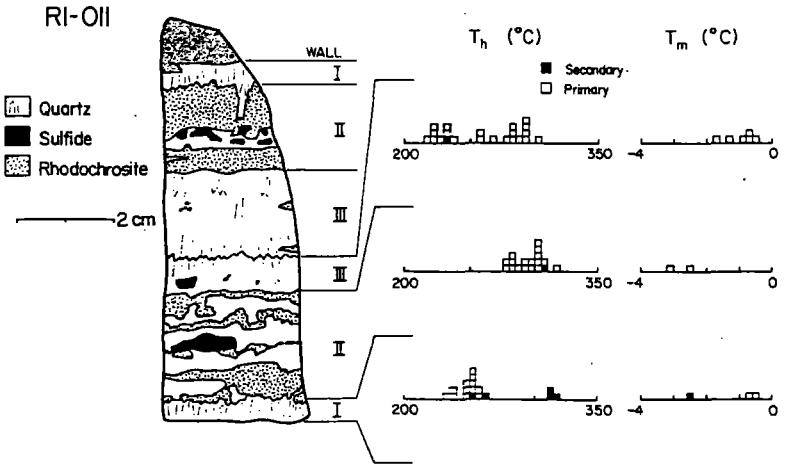

FIG. 5. Sketch of a cross section of sample RI-011 from Newman Hill, showing paragenetic relations among the three zones. Histograms of quartz fluid inclusion homogenization temperatures (T_h) and ice melting point measurements (T_m) are also shown for each of the three zones.

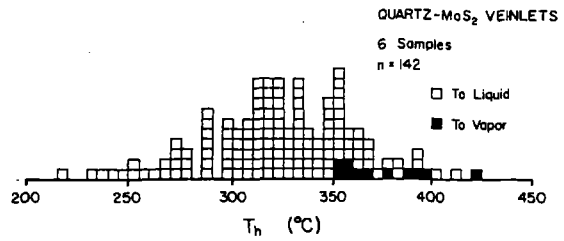

FIG. 6. A histogram showing all homogenization measurements for fluid inclusions from quartz-molybdenite veinlets. Primary inclusions homogenize to either a liquid or a vapor in the temperature range 350° to 420°C. Boiling occurred during deposition in this temperature range.

Hill veins. Zones II and III in both samples yield comparable homogenization temperatures and salinities, but zone I shows distinct variations in both properties. RI-011 shows a thermal maximum during zone II deposition, but RI-023c exhibits a sequential decrease in temperature through the three zones. In both examples zone III yields the lowest average temperature. Fluid salinities (Table 2), calculated using the equations of Potter et al. (1978), follow trends similar to the temperature trends. Fluids from zone II, which contains the sulfide minerals, have salinities of about 4 equiv wt percent NaCl. Zone III salinities in both samples are less than 2.5 equiv wt percent NaCl. RI-011 zone I salinities are about 1 equiv wt percent NaCl, but zone 1 from RI-023c yields the highest salinity of any Newman Hill samples thus far studied (4.25 equiv wt % NaCl). It is possible that the temperature and fluid salinity of zone I deposition vary systematically in Newman Hill veins, but the lack of exposed veins precludes any attempt to map such variations.

Lower and upper Silver Creek

Veins in lower Silver Creek and in the Argentine mine (upper Silver Creek) consist of massive quartz with minor amounts of sulfide minerals, and in lower Silver Creek, magnetite replacing bladed specular hematite. Manganese minerals are absent and the zoning observed on Newman Hill is not present. Euhedral vuggy quartz is present but not abundant. Large inclusions that do not lie in secondary inclusion trains are considered primary and are rare. Secondary inclusions are common as randomly oriented trains that crosscut grain boundaries. No temperature or salinity differences were found between primary and secondary inclusions in any of the samples, although most of the inclusions that were analyzed were clearly of secondary origin. No evidence for boiling was found in any sample. Daughter minerals were not observed. All samples yielded expanded bubbles of carbon dioxide when powders were crushed in oil, but no double menisci were found. Calculated salinities are therefore maximum values. No pressure correction was applied to the lower and upper Silver Creek homogenization data.

Samples from the Argentine mine, RI-015b, RI-015c, RI-017a, and RI-019a, in upper Silver Creek were all collected underground in the Blaine tunnel from the vein that fills the Blackhawk fault. The samples represent 500 m of strike length along the vein. These samples were collected 1.5 km directly above the porphyry molybdenum deposit. K-Ar ages of sericite in the vein walls at this location are 5.39 and 5.45 m.y. (Naeser et al., 1980). These ages place the timing of vein filling within analytical uncertainty of the age of the porphyry mineralization (5.2 m.y., Cameron et al., 1987). Average filling temperatures for these four samples range from 238° to 252°C. The temperatures decrease from southeast to northwest along the fault. Freezing point depressions for these samples all lie between 0° and −0.6°C. These data indicate salinities no greater than 1.05 equiv wt percent NaCl.

Inclusions from only one lower Silver Creek sample, RI-003a, were studied. This sample yielded the lowest average homogenization temperature, 214°C, from the Rico district. Freezing point depressions were not measured for this sample and no daughter minerals were observed. This quartz also probably precipitated from a low salinity fluid, similar to the upper Silver Creek samples.

Sample RI-020 was collected from the dump of the Union Carbonate mine. This mine lies on the northernmost extension of Newman Hill and is 1 km north of the Newman Hill vein system and halfway between the vein system and the Silver Creek molybdenum deposit. This mine is not part of the Newman Hill system because it lacks the characteristic vein zones and the vein does not terminate upward in the Enterprise contact. It resembles more closely the vein samples from the upper Silver Creek area. Vein dump material consists of massive quartz with minor pyrite. Secondary inclusions in one sample, RI-020, yield an average homogenization temperature of 291°C. Freezing point measurements indicate salinities in the range of 1.6 to 3.1 equiv wt percent NaCl. No evidence of boiling and no daughter minerals were found in the inclusions. They did yield expanded carbon dioxide bubbles on crushing in oil, but no double menisci were observed. The calculated salinities are therefore maximum values.

Silver Creek molybdenum deposits

In contrast to the inclusions from the veins, the quartz veinlets in the molybdenum deposit contain

several distinct styles of fluid inclusions. Inclusions from six core samples from two drill holes were examined. Inclusions are abundant in the quartz and occur as unambiguous secondary inclusions in trains that crosscut grain boundaries and as inclusions up to 20 μ in size that commonly exhibit negative crystal shapes. Heating-freezing measurements were restricted to inclusions not in the obvious secondary trains, but the origin of many of the inclusions that were measured cannot be unambiguously defined. The secondary inclusions typically contain a liquid and a gas phase; and about 10 percent also include a euhedral, cubic daughter mineral that is probably halite. Sylvite and an opaque mineral were also observed as daughter minerals. Most of the inclusions not in the obvious trains contain a phase assemblage similar to that in the secondary inclusions. Several of the larger primary inclusions also exhibit double menisci, showing that liquid CO_2 is present. All of the samples produced expanded CO_2 bubbles when powdered quartz was crushed in oil.

Figure 6 summarizes all of the homogenization temperatures for the six core samples. Although most of these inclusions homogenized to a liquid in the range 225° to 415°C, 11 of the inclusions homogenized to a vapor in the temperature range 355° to 425°C. This is clear evidence of boiling in the hydrothermal fluid. No pressure correction is necessary because deposition occurred on the boiling curve. A systematic vertical gradient in average homogenization temperatures was not observed between the two drill holes.

Freezing measurements were restricted to inclusions that did not contain salt daughter minerals. Two types of melting phenomena were observed:

1. Some inclusion fluids melted at temperatures below 0°C, in the range from −0.4° to −4.6°C. Salinities calculated from these data range from 0.61 to 7.22 equiv wt percent NaCl. These salinities are maximum estimates because CO_2 is present.

2. Seven of the inclusions exhibited melting in the range 8.0 to 9.6°C. These inclusions did not exhibit double menisci, but most contained a wide dark zone at the boundary between the liquid and vapor phases in which a sharp contact could not be observed. The high temperatures result from melting of a clathrate (Collins, 1979; Hedenquist and Henley, 1985). Melting phenomena in these inclusions should also include ice and clathrate freezing points below zero, but freezing relationships were difficult to observe because of the dark diffuse nature of the liquid-vapor contact. All of the inclusions with high melting temperatures have homogenization temperatures in the upper range of the histogram in Figure 6.

Homogenization to both liquid and vapor phases in the range 350° to 420°C shows that boiling occurred in the hydrothermal fluid. These temperatures are the highest observed in the porphyry molybdenum samples and are interpreted to represent the actual conditions during initial quartz deposition. Some of the lower homogenization temperatures (Fig. 6) undoubtedly represent secondary inclusions. These data suggest that the temperature of the fluid decreased by about 50°C during later fluid flow in the veinlets.

Oxygen and Hydrogen Isotope Measurements

Oxygen isotope ratios for vein quartz and hydrogen isotope ratios of inclusion fluids from quartz were measured to determine the source of the hydrothermal fluids. The $\delta^{18}O$ values of quartz from veins on Newman Hill, from lower Silver Creek, from the Argentine mine (upper Silver Creek), and from veinlets from the Silver Creek molybdenum deposit were measured. These data are presented in Table 3. Figure 7 compares all the $\delta^{18}O$ values from the Rico district. δD values of inclusion fluids for quartz from Newman Hill, the Argentine mine, and the porphyry molybdenum veinlets were measured and are reported in Table 4.

TABLE 3. The $\delta^{18}O$ Values for Vein and Veinlet Quartz from the Rico District

Sample no.	Location in Figure 3	$\delta^{18}O_{quartz}$
Quartz-molybdenite veinlets		
SC-5 4168	A	+8.4
SC-5 4314	A	+8.6
SC-5 4409	A	+7.5
SC-7a 4681	B	+8.7
SC-7a 4735	B	+8.6
Epithermal veins		
RI-003a	C	−6.1
RI-004a	D	−5.5
RI-011 I	E	+4.7
RI-011 II	E	+4.7
RI-011 III	E	−0.5
RI-012	E	−0.5
RI-014	E	+1.2
RI-015b	F	−4.4
RI-015c	F	−0.9
RI-017a	G	−3.9
RI-019a	H	−3.5
RI-019e	H	−3.4
RI-020	I	−1.5
RI-021	I	−1.5
RI-023c I	J	+2.6
RI-023c II	J	+3.3
RI-023c III	J	+1.6
RI-026f	K	−5.7

All data are per mil relative to SMOW

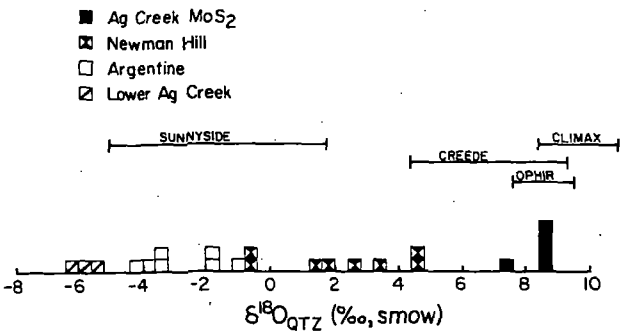

FIG. 7. A histogram of all $\delta^{18}O$ analyses of vein and veinlet quartz from the Rico district. The $\delta^{18}O$ values for quartz from other Tertiary deposits in Colorado are shown for comparison. The range of quartz $\delta^{18}O$ values for porphyry mineralization at Climax (Hall et al., 1974) and in the Ophir (West Silverton) area (Ringrose et al., 1986) are in the same range of values as those for the Silver Creek deposit at Rico. Epithermal vein quartz values at the Sunnyside mine (Casadevall and Ohmoto, 1977) are in the same range as the lower Silver Creek and Argentine quartz samples, but the Creede (Bethke and Rye, 1979) vein quartz values are higher than typical epithermal quartz vein samples.

Oxygen isotope ratios

Figure 7 shows that each of the areas in the Rico district contains quartz that exhibits a distinct range of $\delta^{18}O$ values. Data from each group do not overlap with data from any other group. The massive, weakly mineralized, quartz veins from lower and upper Silver Creek yield the lowest $\delta^{18}O$ values found in the district. Lower Silver Creek values range from −5.5 to − 6.1 per mil. Quartz from the Argentine and Union Carbonate mines have $\delta^{18}O$ values in the range −0.9 to −3.9 per mil. Quartz from the porphyry molybdenum veinlets produced the highest $\delta^{18}O$ values. These data cluster between 7.5 and 8.7 per mil, and with the exception of SC-5 4409, the data lie within the 0.3 per mil range from 8.4 to 8.7 per mil.

Quartz $\delta^{18}O$ values from the Newman Hill veins lie between the Silver Creek vein values and the porphyry veinlet values, from −0.5 to +4.7 per mil. Quartz from each of the three paragenetic zones in samples RI-011 and RI-023c was analyzed. A consistent trend was not found between these two samples. In RI-011 quartzes from zones I and II have identical values of 4.7 per mil, and zone III quartz has a value of −0.5 per mil. In RI-023c the $\delta^{18}O$ values of the quartz vary from 2.6 to 3.3 to 1.6 from zones I through III.

Figure 7 also compares the Rico quartz $\delta^{18}O$ values to values from other vein and porphyry deposits in Colorado. Quartzes from the Sunnyside mine (Casadevall and Ohmoto, 1977), a late Tertiary vein deposit in the western San Juan Mountains, overlap nearly the entire range of vein quartz analyses from Rico. Quartzes from the Creede district (Bethke and Rye, 1979), central San Juan Mountains, yield $\delta^{18}O$ values higher than all but two of the Rico veins. Quartzes from other areas of porphyry molybdenum mineralization (Climax, Hall et al., 1974; Ophir, Ringrose, et al., 1986) have $\delta^{18}O$ values that directly overlap the values from the Silver Creek molybdenum deposit.

Hydrogen isotope ratios

Inclusion fluids from seven samples of quartz were analyzed for hydrogen isotope ratios (Table 4). The δD values for the three paragenetic zones in RI-011 vary from −121 through −117 to −112 per mil for zones I through III. Fluid inclusions from these three zones are predominantly primary, and the secondary inclusions in zone I have been shown to have formed from zone II fluids. The samples for δD analyses were ground to finer than 160 mesh in an attempt to fracture the quartz along zones of secondary inclusions prior to extraction to the fluids for analysis. The hydrogen isotope ratios for each zone are therefore probably derived from predominantly primary inclusions, although some mixing with secondary inclusion fluids could not realistically be avoided. Two samples from the Argentine mine yielded nearly identical δD values of −117 and −113 per mil. The inclusions from these samples were almost entirely secondary in origin.

Two samples of quartz from the molybdenum deposit produced δD values of −90 and −104 per mil, both heavier than any of the vein samples. Primary and numerous secondary inclusions are present in the quartz from the quartz-molybdenite veinlets. Grinding to finer than 160 mesh was again used in an attempt to fracture the quartz along planes of

TABLE 4. The δD Values for Quartz Inclusion Fluids from the Rico District

Sample no.	δD_{water}	$\delta^{18}O_{water}$
Quartz-molybdenite veinlets		
SC-5 4168	−104	+1.5
SC-5 4409	−90	+1.8
Epithermal veins		
RI-011 I	−121	−4.9
RI-011 II	−117	−3.0
RI-011 III	−112	−10.2
RI-017a	−117	−13.7
RI-019a	−113	−12.9

Also shown are $\delta^{18}O$ values for fluids in equilibrium with the quartz calculated from the average homogenization temperatures (Table 1) and the quartz $\delta^{18}O$ values (Table 3) using the quartz-water fractionation equation of Clayton et al. (1972); all data are per mil relative to SMOW

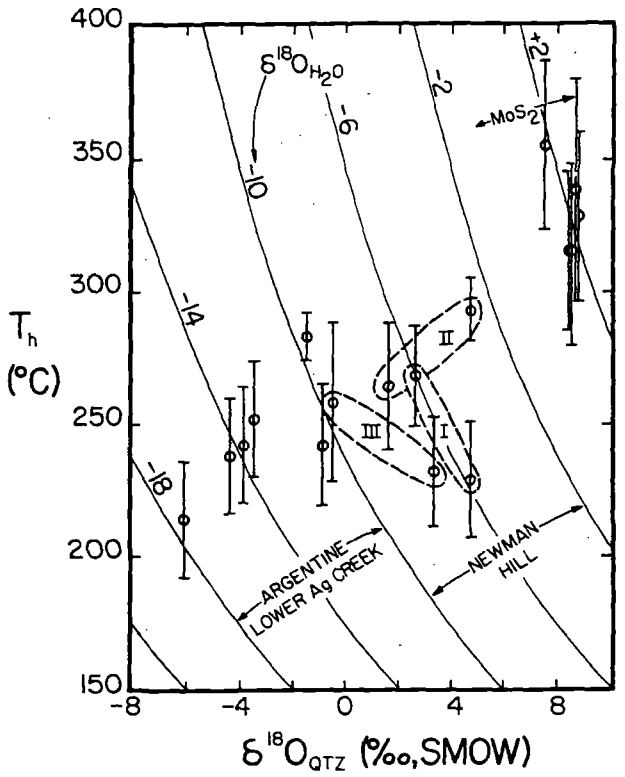

FIG. 8. Plot of average homogenization temperatures (T_h) for fluid inclusions vs. quartz $\delta^{18}O$ values. Also shown are isopleths of $\delta^{18}O$ values for water in equilibrium with quartz calculated using the quartz-water fractionation of Clayton et al. (1972). The vertical bars represent the standard deviation in T_h measurements for each sample. The $\delta^{18}O$ value of water in equilibrium with the quartz for each of the samples can be read directly from the isopleths. The porphyry fluids had consistently high $\delta^{18}O$ values and the lower Silver Creek and Argentine fluids had low values. The Newman Hill fluids are intermediate between the porphyry and massive quartz fluids, but this is not the result of mixing between these two distinct reservoirs. Figure 9 shows that the Newman Hill fluids are typical ^{18}O-shifted meteoric waters and that the porphyry fluids contain a magmatic component.

secondary inclusions and thus exclude these fluids from the analysis. The values of −90 and −104 per mil lie midway between the vein fluid values of about −115 per mil and the magmatic water values of −40 to −80 per mil (Taylor, 1974, 1979).

Origin of the Hydrothermal Fluids

Oxygen isotope values for fluids in equilibrium with quartz in all the samples for which quartz $\delta^{18}O$ values and average homogenization temperatures were measured are shown in Figure 8. This figure plots the quartz $\delta^{18}O$ value versus T_h. Water $\delta^{18}O$ isopleths are also shown. These were calculated using the quartz-water fractionation equation of Clayton et al. (1972). The oxygen isotope values for the hydrothermal fluids fall into three distinct fields in Figure 8. The quartz-molybdenite veinlet fluids have $\delta^{18}O$ values that cluster within 0.5 per mil of 2.0 per mil. The data from the massive quartz veins in lower Silver Creek, the Argentine mine, and the Union Carbonate mine yield water values less than −9 per mil. The Newman Hill veins have water values that are intermediate between the quartz–molybdenite veinlets and the massive quartz veins.

The isotopic compositions of fluids involved in the porphyry and vein mineralization in the Rico district (Fig. 9) can be defined using the hydrogen isotope analyses of the inclusion fluids and the oxygen isotope values of fluids in equilibrium with the hydrothermal quartz (Fig. 8). These data suggest that two fluids with distinct isotopic signatures were responsible for the mineralization. The porphyry fluid probably contained both a magmatic and an ^{18}O-shifted meteoric component. The epithermal fluid was an ^{18}O-shifted meteoric water.

Figure 9 shows the fields of quartz-forming fluids for other mid-Tertiary or younger vein deposits in the San Juan Mountains, including the Sunnyside mine in the Eureka graben (Casadevall and Ohmoto, 1977) and the Mammoth Revenue mine at Platoro (Brooks et al., 1986). Vein quartz fluids from the West Silverton district, 33 km northeast of the Rico district, plot in the same area in Figure 9 (Ringrose et al., 1986). These data show that ^{18}O-shifted meteoric water is a common vein-forming

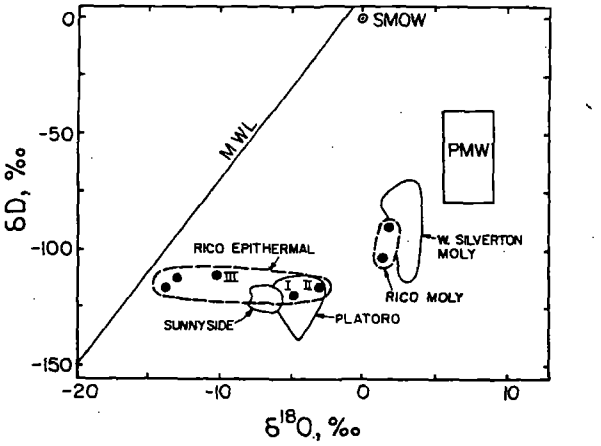

FIG. 9. Plot of δD fluid inclusions vs. calculated $\delta^{18}O$ values of the hydrothermal fluids in the epithermal veins and porphyry veinlets from the Rico district. The meteoric water line (MWL) and the field of primary magmatic water (PMW) (Taylor, 1979) are also shown. The epithermal fluids define the typical ^{18}O-shifted pattern that is characteristic of meteoric-hydrothermal fluids in hot spring and epithermal systems. The porphyry fluid lies on a mixing trajectory between the ^{18}O-shifted epithermal fluid and the field of magmatic water. Also shown are fields of hydrothermal fluid compositions for other Tertiary epithermal vein systems in the San Juan Mountains: the Sunnyside periods I to V (Casadevall and Ohmoto, 1977) and Platoro (Brooks et al., 1986), and for quartz-molybdenite mineralization in the West Silverton district (Ringrose et al., 1986).

fluid in San Juan hydrothermal systems and that the isotopic composition of meteoric water in the San Juans has been relatively constant since mid-Tertiary time. The Rico epithermal vein-forming fluids are thus typical of western San Juan epithermal fluids. One example of vein-forming fluids in the San Juans that does not plot in the common area in Figure 9 has been found in the Creede district. The hydrothermal system at Creede involved a complex mixture of meteoric and magmatic fluids with an additional fluid derived from a closed basin lake in the moat of the Creede caldera (Bethke and Rye, 1979). These authors suggest that isotopic evolution of the lake may account for the heavier hydrogen isotope ratios found in the inclusions in the Creede quartz.

Stable isotope composition of the quartz-molybdenite fluid

In Figure 9, the quartz-molybdenite fluids plot midway between the epithermal vein fluid that exhibits the greatest ^{18}O shift (the Newman Hill fluids) and the primary magmatic water field (Taylor, 1974, 1979). This relationship suggests that the quartz-molybdenite fluids lie on a mixing trajectory between a magmatic water and an ^{18}O-shifted meteoric water. The quartz-molybdenite fluids lie approximately half way between these two end members. Thus, the fluid probably consisted of nearly equal proportions of each component. Figure 9 also shows the field of quartz-forming fluids for mid-Tertiary quartz-molybdenite veinlets in the West Silverton district (Ringrose et al., 1986). This field overlaps the Rico quartz-molybdenite field. Although the number of δD analyses for the Rico veinlets is limited, the correlation between the Rico data and the West Silverton data suggests that the two analyses for the Rico samples are representative. Ringrose et al. (1986) propose a mixed magmatic-evolved meteoric water heritage for the West Silverton quartz-molybdenite fluids. This is the same model that is here proposed for the Rico quartz-molybdenite fluids. The quartz-molybdenite veinlets probably did not form from pure ^{18}O-shifted epithermal-type fluids because δD values for typical mid-Tertiary and younger meteoric-hydrothermal waters in the San Juan Mountains are about 30 per mil lighter than the δD values of the quartz-molybdenite fluids from both the West Silverton and Rico districts (Fig. 9).

Campbell et al. (1984) have constructed a model which shows that the meteoric-hydrothermal fluids with water/rock ratios less than 0.05 would also plot in the area of the quartz-molybdenite veinlets in Figure 9. These fluids would have reacted with a large volume of rock (low water/rock), and the δD and $\delta^{18}O$ values of such fluids would be buffered by δD and $\delta^{18}O$ values of the rock. Campbell et al. used a fresh unreacted igneous rock ($\delta D = -70‰$, $\delta^{18}O = 7.5‰$) in their calculations. Therefore, their low water/rock model applies only to fluids which have been buffered by a rock that has typical magmatic δD and $\delta^{18}O$ values; the fluid would inherit these at a low water/rock ratio. Criss and Taylor (1983) showed that δD values in altered granites in the Idaho batholith are very sensitive to reaction with small amounts of meteoric water. The δD values in biotites from the batholith exhibit nearly complete equilibration with meteoric-hydrothermal fluids even before the $\delta^{18}O$ values of the feldspars are depleted by as much as 1 per mil (corresponding to a water/rock of less than 0.1) due to oxygen exchange with the fluid. To apply Campbell et al.'s model to the Rico quartz-molybdenite fluids would therefore require that these fluids had experienced low water/rock ratios and that the fluids had interacted with rocks which had not undergone any previous water-rock interaction. This is unreasonable for the Rico hydrothermal system because convection of meteoric-hydrothermal fluids was probably initiated when wall rocks were heated during early stages of magmatism, before the magma was emplaced into its final position and crystallized. Even small amounts of interaction between meteoric-hydrothermal fluids and rocks would result in low δD values in the rocks. Later meteoric-hydrothermal fluids would be buffered by rocks that were already in hydrogen isotopic equilibrium with the fluids and the fluids would maintain their initial δD meteoric values. Therefore, although Campbell et al.'s low water/rock model cannot be conclusively eliminated, it requires special circumstances concerning the timing of the quartz-molybdenite mineralization that cannot be demonstrated for either the Rico or West Silverton quartz-molybdenite occurrences. Thus, the mixed magmatic-evolved meteoric fluid is preferred for the quartz-molybdenite veinlet formation.

Stable isotope composition of the epithermal fluids

The fluids from the epithermal veins form a linear array in Figure 9 that is diagnostic of heated meteoric waters in geothermal areas as first defined by Craig (1963). The array of epithermal fluid compositions indicates that no mixing between the epithermal vein fluids and a magmatic fluid occurred in the epithermal environment. The $\delta^{18}O$ values of the fluids exhibit a wide range due to the characteristic ^{18}O shift that results from oxygen exchange between the heated, convectively driven, meteoric fluid and the country rock. Extrapolating the epithermal trend to the meteoric water line shows that the pristine unexchanged meteoric water in the

Rico area had a δD value of −115 per mil and a $\delta^{18}O$ value of −16 per mil during the time of the hydrothermal event about 5 m.y. ago.

The Newman Hill vein-forming fluids have higher $\delta^{18}O$ values than the fluids which produced the vein in the Argentine mine. The Newman Hill fluids have shifted to $\delta^{18}O$ values about 10 per mil higher than pristine meteoric water, but the Argentine fluids are less than 5 per mil higher. The magnitude of the ^{18}O shift is a function of temperature, water/rock ratio, the initial $\delta^{18}O$ value of the fluid, and the oxygen isotope composition of the reacting rocks in the hydrothermal system (Taylor, 1974, 1979). The initial isotopic composition for both vein fluids was identical, and the fluid probably interacted with the same rocks prior to entering the vein flow channels in both areas. The fluid inclusion homogenization data (Table 1), however, show that the Argentine fluids produced veins at lower temperatures than the Newman Hill fluids.

Salinity variations in the fluids

Salinities of the fluids also vary systematically among the three groups of samples; salinity also changes systematically with the oxygen isotope value of the fluid. The fluid inclusion melting point data from Table 2 are summarized in Figure 10 and are plotted versus the calculated fluid $\delta^{18}O$ values (Fig. 8) in Figure 11. The Argentine and Union Carbonate fields in Figure 11 show that the massive quartz vein fluids had low salinities and low water oxygen isotope values. The Newman Hill fluids have higher salinities and higher fluid $\delta^{18}O$ values than the massive quartz vein fluids.

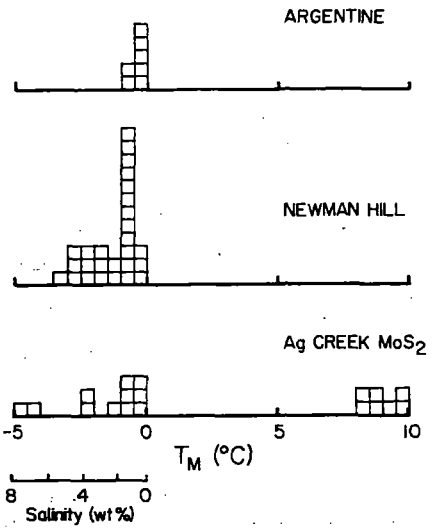

FIG. 10. Histograms comparing the fluid inclusion ice melting temperatures among the three sets of samples. Also shown are the equivalent-weight percent NaCl for these freezing point depressions (Potter et al., 1978). The high melting points observed in some of the porphyry veinlets represent clathrate melting and show that these inclusions contained a high partial pressure of CO_2. See text for further discussion.

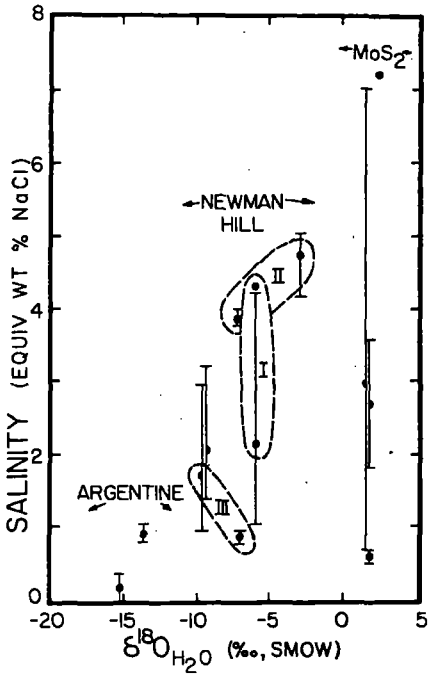

FIG. 11. Plot of fluid inclusion salinity measurements vs. calculated water $\delta^{18}O$ values. The range of salinity measurements for each sample is shown by the vertical bar; the points represent the averages. See text for discussion.

Each of the three paragenetic zones in the Newman Hill veins plot in distinctive locations in Figure 11, although there is some overlap among the three fields. Zone I fluids were intermediate between zone II and III fluids. Zone II fluids have higher salinities and higher $\delta^{18}O$ values than zone I, and zone III fluids have lower salinities and $\delta^{18}O$ values than zone I fluids. The evolution of salinities, fluid $\delta^{18}O$ values, and vein temperatures for the Newman Hill veins are summarized in Figure 12. This figure shows that the mineralized zone II fluids in RI-011 had higher dissolved salts, higher $\delta^{18}O$ values, and formed at higher temperatures than either zone I or III fluids. Zone II must have formed during an influx of a hotter, more saline, more ^{18}O-shifted meteoric water into the Rico vein system. This probably occurred during the peak of thermal activity in the hydrothermal system.

In Figure 11 the quartz-molybdenite fluids plot at high $\delta^{18}O$ values with a wide range of salinities. The Newman Hill fluids lie at an intermediate position between the quartz-molybdenite fluids and the dilute massive quartz vein fluids, but Figure 9 shows that the Newman Hill fluids are not mixtures of these end members. Quartz in the Newman Hill

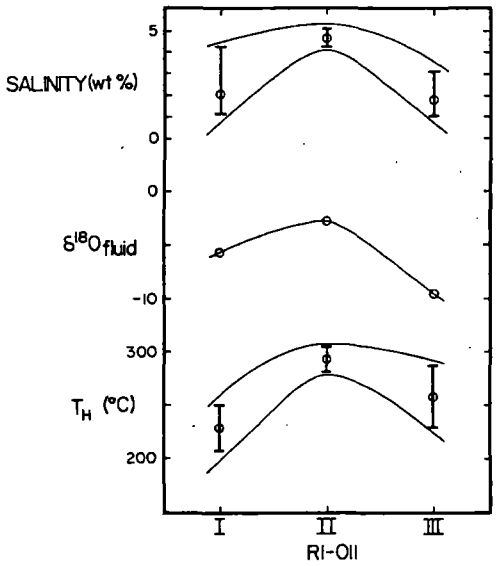

FIG. 12. Evolution of salinity, water $\delta^{18}O$ values, and average fluid inclusion homogenization temperatures for the three paragenetic zones in sample RI-011 from Newman Hill. Figure 5 shows a graphic representation of the paragenetic zoning.

veins precipitated from an evolved, ^{18}O-shifted, meteoric water that contained no detectable magmatic component. Figure 11 indicates that the salinity of the meteoric fluid increased in correlation with the magnitude of the ^{18}O shift.

Evolution of the Hydrothermal Fluids

The δD values of the inclusion fluids and $\delta^{18}O$ values of water in equilibrium with quartz show that an ^{18}O-shifted meteoric fluid was responsible for vein formation on Newman Hill and in lower and upper Silver Creek. A mixed magmatic, ^{18}O-shifted meteoric fluid probably produced the quartz-molybdenite veinlet mineralization in the Silver Creek molybdenum deposit. No evidence for mixing of meteoric and magmatic fluids was found in the epithermal veins. For example, two samples from the Argentine vein, collected 1.5 km directly above the porphyry mineralization from a vein which fills a fault that extends into the center of the highest known grade of molybdenum mineralization, yield water compositions which show no indication of the involvement of magmatic fluids in their formation (Fig. 9). Sericite K-Ar ages show that the vein formed contemporaneously with the molybdenum deposit. No other isotope data from any of the epithermal veins indicate the involvement of a magmatic fluid.

The composition and temperature of the epithermal Newman Hill ^{18}O-shifted meteoric fluid did vary as a function of time (Figs. 6 and 11). Zone II fluids were hotter, more saline, and exhibit greater ^{18}O shifts than either zone I or zone III fluids. Zone II was probably precipitated during the peak of thermal activity in the Rico hydrothermal system. The zone II fluids probably have undergone a greater degree of interaction with rocks prior to entering the Newman Hill fractures than the zone I and III fluids, because the zone II fluids show the greatest ^{18}O shifts. Magmatic fluids did not contribute to the Newman Hill or other epithermal fluids (Fig. 9). The source of the components dissolved in the zone II (and zones I and III) fluids is probably, therefore, the country rocks through which the fluids flowed prior to entering the veins. Figure 11 shows a positive correlation between salinity and the magnitude of the ^{18}O shift for the epithermal fluids. These data suggest that the quantity of dissolved components in the meteoric-hydrothermal fluids is a function of the degree of interaction between that fluid and the country rocks prior to the fluid entering the vein system.

The massive quartz veins in lower Silver Creek, in the Argentine mine, and in the Union Carbonate mine all exhibit minor ^{18}O shifts relative to the Newman Hill veins. The meteoric-hydrothermal fluids that produced these veins also had relatively low salinities, which would a priori be expected because these fluids interacted with the country rocks to a lesser degree than the Newman Hill fluids. However, the massive quartz veins are more widespread than the Newman Hill veins and also occur closer to the presumed heat source for the hydrothermal system (the porphyry deposit). Examination of Figure 1 shows that the Newman Hill veins occur at a structurally high part of the Rico dome, near the apex. Bedding dips away in three directions from the Newman Hill area. The Newman Hill vein fluids had interacted with a large volume of country rock and had probably circulated deeper into the crust than the massive quartz vein fluids. Upon rising convectively, the Newman Hill fluids were channeled up dip and up structures to the structurally higher parts of the dome, whereas less deeply circulated fluids (massive quartz vein fluids) were channeled along shallower structures and were more dispersed.

These relationships have been assembled into a three-stage model for the evolution of the hydrothermal system at Rico:

1. A partially crystallized stock released a magmatic fluid that mixed with an evolved meteoric fluid in approximately equal proportions and produced the porphyry stockwork mineralization. At the same time, the country rocks were being heated by conductive transport of heat out of the crystallizing magma. Circulation of meteoric-hydrother-

mal fluids due to convection probably had begun and may have caused some precipitation of quartz in fractures. Some of the massive quartz veins probably precipitated at this time. The magmatic fluid was apparently diluted by the meteoric fluid to such a degree that its presence cannot be detected in the epithermal vein samples.

2. The scale of convective circulation continued to increase after the release of the magmatic fluid. The hottest meteoric-hydrothermal fluids produced the zoned veins in Newman Hill during this stage. These fluids exhibit the largest ^{18}O shift of any of the meteoric-hydrothermal fluids, indicating that they reacted with a larger relative volume of country rock. These fluids also contain the highest concentration of dissolved components.

3. Retrograde cooling occurred after the peak of hydrothermal circulation in the system. This last stage of hydrothermal activity produced the zone III assemblage on Newman Hill and probably much of the low-temperature massive vein quartz in lower and upper Silver Creek. Influx of meteoric-hydrothermal fluids into the porphyry molybdenum core probably occurred during both stages 2 and 3.

This model is identical in many respects to one proposed by Sheppard et al. (1969, 1971), who studied the stable isotope values of hydrous alteration minerals associated with porphyry deposits in western North America. Similar models were also suggested for several small porphyry-molybdenum prospects in the West Silverton district, 33 km northeast of the Rico district, by Ringrose et al. (1986). Hannah and Stein (1986) recently proposed a general model for Climax-type porphyry deposits in the Colorado mineral belt; the model includes an early magmatic fluid that forms the typical stockwork mineralization and a later meteoric influx into the mineralized zone and is also identical to the one originally suggested by Sheppard et al. (1969, 1971).

Summary and Conclusions

The conclusions of this research are summarized as follows:

1. Two distinct fluid sources fed the Rico hydrothermal system. Oxygen and hydrogen isotope ratios show that a mixed magmatic, ^{18}O-shifted meteoric fluid produced the porphyry molybdenum mineralization. A hydrothermal fluid derived from local meteoric sources was responsible for vein formation in Newman Hill, lower Silver Creek, and the Argentine mine.

2. Extrapolating the ^{18}O-shifted trend of the meteoric-hydrothermal fluids to the meteoric water line shows that meteoric water at the time of hydrothermal activity in the Rico district had a δD value of -115 per mil and a $\delta^{18}O$ value of -16 per mil. Similar meteoric-hydrothermal fluids were responsible for vein formation in several other mid-Tertiary or younger deposits in the San Juan Mountains, including the Sunnyside mine (Casadevall and Ohmoto, 1977) and the Mammoth-Revenue mine (Brooks et al., 1986), and in the West Silverton district (Ringrose et al., 1986).

3. Three paragenetic zones have been recognized in the Newman Hill veins. Zones I and III are primarily barren quartz. Zone II contains quartz with abundant rhodochrosite and base metal sulfide minerals. Silver sulfide minerals are also found in zone II and provided the economic proportion of the veins. Salinities, $\delta^{18}O$ values, and homogenization temperatures for zones I and III were lower than for zone II. Zone II fluids experienced the largest ^{18}O shift of any vein fluids and had a larger concentration of dissolved components than the zone I and III fluids. The zone II fluids may also have boiled prior to formation of the veins at their present level of exposure. No evidence of a magmatic component was found in any of the epithermal veins.

4. Massive barren quartz veins in lower Silver Creek and in the Argentine and Union Carbonate mines (upper Silver Creek) formed from meteoric-hydrothermal fluids that had lower salinities, lower homogenization temperatures, and smaller ^{18}O shifts than the Newman Hill fluids. No evidence of a magmatic component was found in any of the barren quartz veins, even though the Argentine vein lies directly above the porphyry molybdenum mineralization and fills a fault that is a direct plumbing channel to the porphyry mineralized area.

5. Fluid inclusion homogenization to both a liquid and a vapor shows that boiling occurred at some time in the history of the porphyry mineralization. The temperature of boiling was in the range 350° to 420°C, indicating a pressure during quartz deposition of about 130 bars. The porphyry mineralization occurred early in the history of the Rico system. Numerous trains of lower temperature dilute secondary inclusions in the veinlet quartz suggest a late-stage influx of meteoric-hydrothermal fluids.

Acknowledgments

The ghost of the Anaconda Minerals Company is gratefully acknowledged for providing access to the Rico district and core. Don Cameron and John Wilson were particularly helpful. Kathryn Bailey and Jeff Brooks helped with the fluid inclusion analyses. Hugh Taylor kindly provided access to his lab for the oxygen isotope analyses and Jim O'Neil graciously allowed the use of his lab for the deuterium analyses. Thoughtful discussions with Don Cameron, Jeff Brooks, Kathryn Bailey, and Skip Cun-

ningham provided stimulating input into this paper. Don Cameron and Skip Cunningham reviewed early versions of this manuscript. A Washington State University grant-in-aid provided partial support for this research.

October 29, 1986; March 10, 1987

REFERENCES

Bastin, E. S., 1922, Silver enrichment in the San Juan Mountains, Colorado: U. S. Geol. Survey Bull. 735-D, p. 65–129.

Bethke, P. M., and Rye, R. O., 1979, Environment of ore deposition in the Creede mining district, San Juan Mountains, Colorado: Part IV. Source of fluids from oxygen, hydrogen, and carbon isotope studies: ECON. GEOL., v. 74, p. 1832–1851.

Brooks, J. W., Larson, P. B., and O'Neil, J. R., 1986, Paragenesis and fluid characteristics of the Mammoth Revenue vein, Platoro caldera, San Juan Mountains, Colorado [abs.]: Geol. Soc. America, Abstracts with Programs, v. 18, p. 550.

Cameron, D. C., Barrett, L. F., and Wilson, J. C., 1987, Discovery of the Silver Creek molybdenum deposit, Rico, Colorado: Am. Inst. Mining Metall. Petroleum Engineers Trans., in press.

Campbell, A., Rye, D., and Petersen, U., 1984, A hydrogen and oxygen isotope study of the San Cristabal mine, Peru: Implications of the role of water to rock ratio for the genesis of wolframite deposits: ECON. GEOL., v. 79, p. 1818–1832.

Casadevall, T., and Ohmoto, H., 1977, Sunnyside mine, Eureka mining district, San Juan County, Colorado: Geochemistry of gold and base metal ore deposition in a volcanic environment: ECON. GEOL., v. 72, p. 1285–1320.

Clayton, R. N., O'Neil, J. R., and Mayeda, T. K., 1972, Oxygen isotope exchange between quartz and water: Jour. Geophys. Research, v. 77, p. 3057–3067.

Collins, P. L. F., 1979, Gas hydrates in CO_2-bearing fluid inclusions and the use of freezing data for estimation of salinity: ECON. GEOL., v. 74, p. 1435–1444.

Craig, H., 1963, Isotopic variations in meteoric waters: Science, v. 133, p. 1702–1703.

Criss, R. E., and Taylor, H. P., Jr., 1983, An $^{18}O/^{16}O$ and D/H study of Tertiary hydrothermal systems in the southern half of the Idaho batholith: Geol. Soc. America Bull., v. 94, p. 640–663.

Cross, W., and Ransome, F. L., 1905, Description of the Rico quadrangles: U. S. Geol. Survey Geol. Atlas, Folio 130, 20 p.

Cross, W., and Spencer, A. C., 1900, Geology of the Rico Mountains, Colorado: U. S. Geol. Survey 21st Ann. Rept., pt. 2, p. 7–165.

Haas, J. L., Jr., 1971, The effect of salinity on the maximum thermal gradient of a hydrothermal system at hydrostatic pressure: ECON. GEOL., v. 66, p. 940–946.

Hall, W. E., Friedman, I., and Nash, J. T., 1974, Fluid inclusion and light stable isotope study of the Climax molybdenum deposits, Colorado: ECON. GEOL., v. 69, p. 884–901.

Hannah, J. L., and Stein, H. J., 1986, Oxygen isotope compositions of selected Laramide-Tertiary granitoid stocks in the Colorado mineral belt and their bearing on the origin of Climax-type granite-molybdenum systems: Contr. Mineralogy Petrology, v. 93, p. 347–358.

Hedenquist, J. W., and Henley, R. W., 1985, The importance of CO_2 on freezing point measurements of fluid inclusions: Evidence from active geothermal systems and implications for epithermal ore deposition: ECON. GEOL., v. 80, p. 1379–1406.

Larson, P. B., and Taylor, H. P., Jr., 1987, Solfataric alteration in the San Juan Mountains, Colorado: Oxygen isotope variations in a boiling hydrothermal environment: ECON. GEOL., v. 82, p. 1019–1038.

Matsuhisa, Y., Morishita, Y., and Sato, T., 1985, Oxygen and carbon isotope variations in gold-bearing hydrothermal veins in the Kushikino mining area, southern Kyushu, Japan: ECON. GEOL., v. 80, p. 283–293.

McKnight, E. T., 1974, Geology and ore deposits of the Rico district, Colorado: U. S. Geol. Survey Prof. Paper 723, 100 p.

Naeser, C. W., Cunningham, C. G., Jr., Marvin, R. F., and Obradovich, J. D., 1980, Pliocene intrusive rocks and mineralization near Rico, Colorado: ECON. GEOL., v. 75, p. 122–127.

O'Neil, J. R., Silberman, M. L., Fabbi, B. P., and Chesterman, C. W., 1973, Stable isotope and chemical relations during mineralization in the Bodie mining district, Mono County, California: ECON. GEOL., v. 68, p. 765–784.

Potter, R. W., II, 1977, Pressure corrections for fluid-inclusion homogenization temperatures based on the volumetric properties of the system NaCl-H_2O: U. S. Geol. Survey Jour. Research, v. 5, p. 603–607.

Potter, R. W., II, Clynne, M. A., and Brown, D. L., 1978, Freezing point depression of aqueous sodium chloride solutions: ECON. GEOL., v. 73, p. 284–285.

Pratt, W. P., McKnight, E. T., and DeHon, R. A., 1969, Geologic map of the Rico quadrangle, Dolores and Montezuma Counties, Colorado: U. S. Geol. Survey Geol. Quad. Map GQ-797.

Ransome, F. L. 1901, The ore deposits of the Rico Mountains, Colorado: U. S. Geol. Survey 22nd Ann. Rept., pt. 2, p. 229–398.

Ringrose, C. R., Harmon, R. S., Jackson, S. E., and Rice, C. M., 1986, Stable isotope geochemistry of a porphyry-style hydrothermal system, West Silverton district, San Juan Mountains, Colorado, USA: Appl. Geochemistry, v. 1, p. 357–373.

Robinson, B. W., and Christie, A. B., 1980, Epithermal silver-gold mineralization, Maratoto mine, New Zealand: Stable isotopes and fluid inclusions, *in* Ridge, J. D., ed., Proceedings of the fifth quadrennial IAGOD symposium, vol. 1: Stuttgart, E. Schwizerbart'sche, p. 719–730.

Rye, R. O., and Sawkins, F. J., 1974, Fluid inclusion and stable isotope studies on the Casapalca Ag-Pb-Zn-Cu deposit, central Andes, Peru: ECON. GEOL., v. 69, p. 181–205.

Sheppard, S. M. F., and Gustafson, L. B., 1976, Oxygen and hydrogen isotopes in the porphyry copper deposit at El Salvador, Chile: ECON. GEOL., v. 71, p. 1549–1559.

Sheppard, S. M. F., Nielsen, R. L., and Taylor, H. P., Jr., 1969, Oxygen and hydrogen isotope ratios of clay minerals from porphyry copper deposits: ECON. GEOL., v. 64, p. 755–777.

—— 1971, Hydrogen and oxygen isotope ratios in minerals from porphyry copper deposits: ECON. GEOL., v. 66, p. 515–542.

Taylor, H. P., Jr., 1973, O^{18}/O^{16} evidence for meteoric-hydrothermal alteration and ore deposition in the Tonopah, Comstock lode, and Goldfield mining districts, Nevada: ECON. GEOL., v. 68, p. 747–764.

—— 1974, The applications of oxygen and hydrogen isotopes studies to problems of hydrothermal alteration and ore deposition: ECON. GEOL., v. 69, p. 843–883.

—— 1979, Oxygen and hydrogen isotope relationships in mineral deposits, *in* Barnes, H. L., ed., Geochemistry of hydrothermal ore deposits: New York, Wiley Intersci., p. 236–277.

Taylor, H. P., Jr., and Epstein, S., 1962, Relationship between O^{18}/O^{16} ratios in coexisting minerals in igneous and metamorphic rocks. Part 1. Principles and experimental results: Geol. Soc. America Bull., v. 73, p. 461–480.